Influence of inherited basement structures on the active Sumatran Fault and Volcanic Arc, Indonesia

Lukman sutrisno[1], Jeroen Smit[2], Damien Bonté[3], Yunus Daud[4], Fred Beekman[5], Widodo Purwanto[6], and Jan Diederik van Wees[7]

[1]Department of Earth Sciences, Faculty of Geosciences, Universiteit Utrecht
[2]Utrecht University
[3]Department of Earth Sciences, Faculty of Geosciences, Universiteit Utrecht (Presently at IFP Energies Nouvelles, France)
[4]Faculty of Mathematics and Natural Sciences, Universitas Indonesia
[5]University of Utrecht
[6]Faculty of Engineering, Universitas Indonesia
[7]TNO

November 24, 2022

Abstract

We present a novel tectonic and structural framework for the Sumatran Volcanic Arc and Sumatran Fault System (SFS), based on a comprehensive compilation of the controls of heterogeneities in both subducting and overriding plate on the local to lithospheric-scale geology. A new conceptual model is proposed to explain the interaction between pre-existing inherited basement structures, which are well exposed along the arc, with the much younger SFS. The model also illustrates the relationship between brittle deformation and nearby magmatism-volcanism. We present a novel structural restoration of the island prior to the SFS strike-slip faulting contributing to in-depth understanding of the initial condition of the island, especially in view of the basement structures underlying the volcanic arc and the inherited basement structures. More detailed structural analysis along the SFS showcases different interaction styles between SFS and the basement structures. Different intersection angles between those two structural features create different deformation styles along the arc. An elongated rhomboidal pull-apart basin is expected where the segments of SFS are parallel or sub-parallel to the basement structures, while a more complex and irregular pull-apart basin is developed where the intersection angle is larger. The structural controls on volcanism along the arc are located along the basement structures, and demonstrate that they are only partially in tune with the SFS fault structures. Furthermore, the different deformation styles and interaction between volcanism-tectonism along the arc have been grouped into two different main tectono-volcanic domains, with distinctive transitional area around the Toba Caldera Complex.

Influence of inherited basement structures on the active Sumatran Fault and Volcanic Arc, Indonesia

Lukman Sutrisno[1], Jeroen Smit[1], Damien Bonté[1*], Yunus Daud[2], Fred Beekman[1], Widodo Purwanto[3], Jan Diederik Van Wees[1,4]

[1] Department of Earth Sciences, Faculty of Geosciences, Universiteit Utrecht, The Netherlands

[2] Faculty of Mathematics and Natural Sciences, Universitas Indonesia, Indonesia

[3] Faculty of Engineering, Universitas Indonesia, Indonesia

[4] TNO, The Netherlands

[*] Presently at IFP Energies Nouvelles, France

Corresponding author: l.sutrisno@uu.nl

Keywords

basement structure, oblique subduction, pull-apart basin, restraining bend, strike-slip, Sumatran Fault System, transpressional, transtensional, volcano

Abstract

We present a novel tectonic and structural framework for the Sumatran Volcanic Arc and Sumatran Fault System (SFS), based on a comprehensive compilation of the controls of heterogeneities in both subducting and overriding plate on the local to lithospheric-scale geology. A new conceptual model is proposed to explain the interaction between pre-existing inherited basement structures, which are well exposed along the arc, with the much younger SFS. The model also illustrates the relationship between brittle deformation and nearby magmatism-volcanism. We present a novel structural restoration of the island prior to the SFS strike-slip faulting contributing to in-depth understanding of the initial condition of the island, especially in view of the basement structures underlying the volcanic arc and the inherited basement structures. More detailed structural analysis along the SFS showcases different interaction styles between SFS and the basement structures. Different intersection angles between those two structural features create different deformation styles along the arc. An elongated rhomboidal pull-apart basin is expected where the segments of SFS are parallel or sub-parallel to the basement structures, while a more complex and irregular pull-apart basin is developed where the intersection angle is larger. The structural controls on volcanism along the arc are located along the basement structures, and demonstrate that they are only partially in tune with the SFS fault structures. Furthermore, the different deformation styles and interaction between volcanism-tectonism along the arc have been grouped into two different main tectono-volcanic domains, with distinctive transitional area around the Toba Caldera Complex.

1. Introduction

Oblique subduction causes strain partitioning in subduction zones (*Chemenda et al., 2000; McCaffrey et al., 2000*), typically by concentrating the compressional component along the trench and the transcurrent component further inland, for some cases in or nearby the volcanic arc (*Schutt and Whip, 2020; Seymour et al., 2020*). The influence of inherited/ older basement structures on the younger transcurrent faulting and arc volcanism has been advocated for several of these oblique subduction systems. Located along the long-lived active margin of Sundaland, Sumatra is the product of a long history of overall plate convergences since the Paleozoic, involving the repeated subductions, volcanism, and terrane accretions. Some authors (*Pulunggono et al., 1992; Hutchison, 1993*) have pointed to the importance of long-lived inherited structures from previous plate interaction controlling later stage lithospheric scale and crustal deformation, but still a comprehensive tectonic framework in terms of structural inheritance is lacking.

Such a framework would allow a more robust structural interpretation of lithosphere deformation by local scale geodynamic models, and provide an in-depth understanding of the geodynamic evolution of Sumatra in view of the deformational and crustal complexity. This is of high relevance for geological understanding and provides important conceptual input for constraining the predictive models for formation and containment of earth resources in sedimentary and crystalline basement rocks, such as geothermal, mineral deposit, and hydrocarbons.

This paper reviews the controls of long-lived heterogeneities in the incoming plate, subducted slab, and overriding plate on the local- to lithospheric-scale geology, explaining the observed contrasts in deformation styles. Based on the analysis of local and regional geology and active deformation, fault kinematics, and also collocated magmatism-volcanism, we propose a new conceptual models to explain the interaction between pre-existing inherited basement structures with the currently active Sumatra Fault System (SFS). This model explains the observed contrasting deformation styles in the northern and southern part of the arc, including the transition domain in the central part. The model also provides a better understanding in the relationship between brittle deformation and the nearby magmatism-volcanism.

A compilation of the large scale features in both the incoming plate and subducted slab, and the overriding plate presented in Section-2 provides the framework for a more detailed structural analysis of basement structures and the SFS structural style in Section-3 and 4, respectively. Section-3 presents a novel structural restoration of the island prior to the strike-slip faulting contributing to in-depth understanding of the initial condition of the island, especially in view of the basement structures underlying the volcanic arc and the inherited basement structures. Subsequently, in Section-4 a more detailed structural analysis is presented, showcasing different interaction styles between SFS and the basement structures determined by the intersecting angle between those two structural features. In addition, we discuss in detail in Section-5 the implications of our revised structural interpretation of Sumatra in view of structural controls on volcanism along the arc which are located along the basement structures, and demonstrate that they are only partially in tune with the SFS fault structures. Furthermore, the different deformation styles and interaction between volcanism-tectonism along the arc have been grouped into three different tectono-volcanic domains.

2. Tectonic framework of Sumatran subduction zone

Sumatra is the western most major island of the Indonesian Archipelago. Oriented NW-SE, Sumatra stretches over more than 1600 km, with a maximum width that exceeds 350 km. Indian Ocean subduction trench that is located about 250 km to the southwest of Sumatra marks the deformation front of the active subduction zone which run over the full length of the island. An accretionary wedge and fore-arc basins separate the trench from the mainland Sumatra. The inland volcanic arc and the alluvial plain dominate the physiography of the island (Figure-1). As a backbone of the island, the arc system of more than 30 Quaternary volcanic complexes forms a prominent topographic high. The volcanic complexes partly cover the uplifted and exposed pre-Tertiary basement and the Tertiary formations, including pre-Quaternary volcanic rocks. In contrast, relatively flat topography of the alluvial plain that covers older sedimentary basins dominates north eastern Sumatra between the arc and the Malaka Strait.

Sumatra is located at the south-western margin of Sundaland. Consequently, Sumatra's Phanerozoic geological history is closely related to Sundaland's geodynamic evolution. As a southern promontory of the Eurasian landmass (*Hall and Morley, 2004*), most of Sundaland was constructed by amalgamation of Gondwana-derived tectonic blocks during the Early Mesozoic (*Hutchison, 1994; Metcalfe, 2011*). The repeating cycles of subduction, accretion, and the initiation of new subduction systems happened since the Late Permian (*Metcalfe, 2000; Barber and Crow, 2003; Hall, 2012*). The large-scale tectonic features of Sumatra are oriented sub-parallel to the Island's current long axis of which the orientation differs from the orientation of the accreted terranes that form the basement of Sumatra. They are known from gravimetry and outcrops that are largely concentrated along the SFS (Figure-1 and 2).

The Pre-Tertiary basement underlying most of the south-western part of Sundaland contains Carboniferous-Permian sediments deposited on continental terranes. These deposits formed before their amalgamation to the core of Sundaland in Late Permian to Early Triassic times (*Hall, 2002; Barber and Crow, 2003*), and the amalgamation of terranes progressed up to the Middle Cretaceous (*Barber and Crow, 2003*). Afterwards, the latest subduction began following the accretion of the last tectonic entity i.e., Woyla Block (*Advokaat et al., 2018*).

The subduction system along the southern margin of Sumatra was initiated in Mid Eocene (45 Ma) (*Hall, 2002; Hall and Spakman, 2015*). During the Oligocene, the geology of Sumatra is characterized by the widespread development of basins (*Davies, 1984, Howles Jr., 1986;*

Pulunggono, 1986; Moulds, 1989; Heidrick and Aulia, 1993) and simultaneous subduction-related magmatism and volcanism (*Barber and Crow, 2005*). Formation of the dextral SFS due to oblique convergence took place from the Miocene (13 Ma), accompanied by regional uplift and inversion of all the sedimentary basins to the Pliocene-Pleistocene (*Eubank and Makki, 1981, Williams and Eubank, 1995; McCarthy and Elders, 1997; Sieh and Natawidjaja, 2000*). Quaternary volcanism completes the Sumatran geology (*Gasparon and Verne, 1998*).

In contrast with Borneo, a recent paleomagnetic study suggests that Sumatra did not experience significant Cenozoic rotation (*Advookat et al., 2018*). Consequently, since its initiation in Mid Miocene Sumatran subduction system had evolved under an oblique convergence. The neotectonics of Sumatran subduction system has been summarized by many authors (*McCaffrey, 1991; McCaffrey, 2009*), including GPS observation (*Genrich et al., 2000; Prawirodirdjo et al., 2010*), seismicity (*Lange et al., 2010*), and associated strain partitioning (*Sieh and Natawidjaja, 2000; Bradley et al., 2017*). The variation of deformation styles observed along Sumatran Arc has been ascribed to heterogeneities in the incoming plate and the subducted slab on one hand and the overriding plate on the other hand (*Barber and Crow, 2005; Hall and Morley, 2004; Pubellier et al., 2014; Zahirovic et al., 2014; Hall and Spakman, 2015*). Below we analyse these controls.

2.1. The subducting plate

Series of north-south regional fracture zones compartmentalize the incoming Indian oceanic plate, as indicated by free-air gravity derived seafloor topography (*Smith and Sandwell, 1997*) (Figure-1A). The most prominent features are Ninety-East Ridge and Investigator Fracture Zone (IFZ), both remnants of now inactive transform faults (*McKenzie and Sclater, 1971*;

Jacob et al., 2014). The IFZ is closer and thus more relevant for Sumatran subduction system. The overall shallower depth of the ocean floor in the western side of IFZ may result from the distal Ganges submarine fan, the IFZ ridge seems to act as a barrier that prevents Ganges fan to extend even further to the south-eastern (*Barber and Crow, 2005*).

Ages of the oceanic lithosphere have been revisited by Jacob et al. (*2014*). It is shown that the IFZ separates several inactive spreading centres and relatively young lithosphere (<60 Ma) in its western side from an older lithosphere (>60 Ma) in the eastern side of the ridge. Weak rheology of the inactive spreading centres surrounded by lighter and younger oceanic lithosphere resists subduction, leading to a landward deflection of the trench (*Jacob et al., 2014*), and to a shallower slab in the northern part of Sumatra (*Pesicek et al., 2008; Hall and Spakman, 2015; Raghuram et al., 2018*). Conversely, the older oceanic lithosphere subducting beneath southern Sumatra has a steeper angle (Figure-1B). The continuation of IFZ into the subducted slab as imaged by seismic tomography is interpreted either as a bend (*Fauzi et al., 1996*) or tearing of the slab (*Hall and Spakman, 2015; Koulakov et al., 2016*). Both interpretations are based on the anomalous magmatism of Toba Caldera Complex which is located right above the slab irregularities (*Fauzi et al., 1996; Koulakov et al., 2016*).

Strong stress field variations within the incoming plate due to age difference of oceanic plate (*Cloetingh and Wortel, 1986*) suit well with the latest kinematic study of Sumatran subduction system, which suggests diffuse deformation within the Indian oceanic plate, in contrast to a rigid overriding lithosphere (*Bradley et al., 2017*). Cloetingh and Wortel (*1986*) indicated a net resistance at the convergence zone along the Sumatran subduction system, contrary to the slab pull in the subduction segment in the south of Java and Lesser Sunda. This interpretation is supported by buckling and flexural bulging of the incoming plate in the western side of trench (*Raghuram et al., 2018*).

2.2. The overriding plate

As mentioned earlier, the overriding plate are constructed by amalgamation of Palaeozoic terranes linked by sutures (*Pulunggono and Cameron, 1984; Hutchison, 1994; Barber and Crow, 2003, 2009*) (Figure-1A, 1C, and 2A). These terranes drifted northward in piecemeal during successive Wilson cycles that involved the Paleo-, Meso-, and Neo Tethys oceans (*Barber, 2000; Metcalfe, 2000; Barber and Crow, 2003; Hall, 2002; 2012; Zahirovic et al., 2014; Advokaat et al., 2018*). Based on heat flow, active deformation history, and deep lithospheric structures, Hall and Morley (*2004*) suggest that instead of being a stable cratonic shield, Sundaland, especially the Sumatra region as its margin, acted as thin and relatively hot, thus weak lithosphere.

Sibumasu Terrane dominates the northern half of Sumatra. It was under-thrusted beneath the East Malaya/ Indochina Block following the closing of Paleo Tethys in Middle Permian times (*Barber and Crow, 2003*). The resulting Bentong-Raub Suture Zone (*Metcalfe, 2000*) runs along the central and southern part of eastern coastline, including offshore islands in Malaka Strait. The Bentong-Raub Suture Zone is represented by the tin-bearing granitic belt of Main Range of Malay Peninsula (*Metcalfe, 2000; Barber and Crow, 2003; 2009*). According to Barber and Crow (*2003*), the Medial Sumatra Tectonic Zone (MSTZ) is a currently inactive crustal-scale structure that acted as a regional sub-vertical dextral transcurrent fault during the emplacement of West Sumatra Terrane against Sibumasu Terrane. MSTZ is manifested by a narrow highly deformed band of a rock assemblage from surrounding Palaeozoic basement rocks, low grade metamorphic rocks, and syn-tectonic granitoid. West Sumatra Terrane which dominates the southern half of Sumatra is distinguished from Sibumasu on the basis of Carboniferous fauna (*Fontaine and Gafoer, 1989*). Then Woyla Terrane constitutes most of the western side of Sumatra. It was accreted to Sibumasu and West Sumatra Terranes during

Late Cretaceous (*Barber, 2000*). The Woyla is composed of a volcanic-arc assemblage and an associated oceanic assemblage (*Barber, 2000*) (Figure-1C). To summarize, considering its nature and origin, it is reasonable to think that both Sibumasu and West Sumatra Terrane are continental crust, while Woyla Terrane is a remnant of a volcanic chain formed on top of oceanic crust (Figure-1C).

2.3. The Sumatra Arc and the Sumatran Fault System (SFS)

The Sumatran arc is a prominent topographic high, known as Barisan Mountains, where the Palaeozoic-Mesozoic basement rocks have been uplifted and exposed to the surface (Figure-2A) following Middle Miocene uplift. A major unconformity in the fore-arc region marks this uplift (*Simandjuntak and Barber, 1996; McCarthy and Elders, 1997*). Indeed, the tectonic blocks underlying Sumatra in Figure-1A and 1C have been interpreted from various Pre-Tertiary outcrops along Barisan Mountains (Figure-2A). The Barisan Mountains runs through the whole island and in general coincides with the modern volcanic arc (Figure-2A). In the southern half of the island the Barisan Mountains are relatively narrow and the uplifted Pre-Tertiary basements and Tertiary units are largely covered by the Quaternary volcanic products. Toward its northern end the Barisan Mountains get slightly wider and, except around Toba Caldera, the Quaternary volcanics are relatively less widespread so that the basement structural expression appears more obvious over a broader area (Figure-2A and -3).

Intra-arc deformation along the Sumatran Arc is currently dominated by dextral strike-slip faulting along the Sumatra Fault System (SFS). However, compressional deformation had also reactivated the basement structures, caused significant uplift forming the Barisan Mountains, exposing and eroding Palaeozoic-Mesozoic basement and Tertiary cover. The study of present-day stress orientation around SFS suggests that crustal-scale strike-slip faults in general are inherently weak surfaces (*Mount and Suppe, 1992*), thus decoupling between strike-slip and compressional component takes place within a broadly transpressive deformation due to oblique convergence.

The NW-SE oriented dextral strike-slip SFS is one of the most marked and studied tectonic features in Sumatra. In a geodynamic context, the SFS accommodates most of the strike-slip component of the oblique subduction beneath Sumatra (*McCarthy and Elders, 1997; McCaffrey et al., 2000; McCaffrey, 2009*). It connects the opening of the Andaman Sea north west of Sumatra and the vast transtensional deformation of Sunda Strait, south east of Sumatra. It separates the north-westward moving rigid fore-arc sliver from the relatively stable Sundaland by dextral strike-slip rate of 15-16 mm/year (*Bradley et al., 2017; Natawidjaja et al., 2017*). McCarthy and Elders (*1997*) postulate that the Sumatran Arc, known as Barisan Mountains, and the SFS were initiated at the same time around the Middle Miocene (±13 Ma). Other authors suggest a much younger age especially for the southern segment of the fault assuming significant trench-parallel extension in the fore-arc sliver (*Sieh and Natawidjaja, 2000*). However, timing for the onset of formation of the Barisan Mountains, thus including the SFS, is poorly constrained and only deducted indirectly from other information, such as the formation of fore-arc ridges in offshore Sumatra (*Beaudry and Moore, 1985*), therefore certain degree of uncertainty is still remaining.

Surface traces of the SFS are mostly based on topographic expressions such as lineaments and offsets, with few data directly derived from field observation due to discontinuous and patchy outcrops (*Sieh and Natawidjaja, 2000; Hickman et al., 2004; Natawidjaja et al., 2017; Mukti, 2018; Aribowo, 2018*). The fault's surface traces contain many irregularities, such as curvatures and bends that accommodate local transtension and transpression in the form of pull-apart basins and restraining bends (*Huchon and Le Pichon, 1984; Bellier and Sebrier, 1994; Sieh and Natawidjaja, 2000; Muraoka et al., 2010*) with a variety of geometries.

Locally, the fault zone bifurcates into two or more strands. The most striking split is the fault's northern end (*Fernandez-Blanco et al.,* 2016) and southern end near the Sunda Strait (*Mukti, 2018*), and the Equatorial Bifurcation (EB) in the central part (*Natawidjaja, 2018; Sahara et al., 2018*).

The total right-lateral offset of the SFS has been estimated based on the opening amount of Andaman Sea and the extension of Sunda Strait, and the observable offsets of river channels, geological features, geochemical and geophysical anomalies, and volcanic lineaments (*Katili and Hehuwat, 1967; Posavec et al., 1973; Page et al., 1979; Curray et al., 1979; Huchon and Le Pichon, 1984; McCharty and Elders, 1997; Sieh and Natawidjaja, 2000*). The understanding of the kinematics of SFS has improved further over the past decades through seismicity and geodetic observation and modelling (*Nishimura et al., 1986; McCaffrey, 1991; Prawirodirdjo et al., 1997; Genrich et al., 2000; Chlieh et al., 2008; Lange et al., 2010; Weller et al., 2012; Burton and Hall, 2014; Bradley et al., 2017*).

3. Structural analysis of the Sumatran Arc

3.1. Data and methods

For multi scale interpretation of the geologic features along the Sumatran arc i.e. the volcanic complexes, the SFS, and the basement structures, as a first step, we performed a structural compilation of 43 geologic maps in 1:250,000 scale published by Indonesian Geological Research and Development Center, and other published maps (*Posavec et al., 1973; Aldiss and Ghazali, 1984; Huchon and Le Pichon, 1984; Bellier and Sebrier, 1994; McCarthy and Elders, 1997; Sieh and Natawidjaja, 2000; Barber and Crow, 2005; Muraoka et al., 2010; Nukman and Moeck, 2013; Fernandez-Blanco et al., 2015; Berglar et al., 2017; Bradley et al., 2017; Natawidjaja et al., 2017; Natawidjaja, 2018; Aribowo, 2018*). Subsequently, the structural compilation has been complemented by morphologic observation and interpretation of a digital elevation model with 0.27 arc-second resolution (*http://tides.big.go.id/DEMNAS*).

In addition, regional gravimetry (*Sandwell and Smith, 2009*), seismicity (*USGS earthquake catalogue, 1960-2019*), the occurrence of thermal anomalies, such as hot springs, fumaroles, and solfatara, and alteration grounds, or lineament of domes are compiled to validate the interpretation of regional lineaments. However, as commonly the case for tropical volcanic terrain, a detailed structural setting of intra-arc features, such as for instance continuation of fault traces, step-overs and bending, or splays are difficult to pin point in the field, due to intensive erosion and coverage of young volcanic rocks over large portion of the arc. Complementing subsurface data for intra-arc structural analysis are mainly available from the sparse geothermal exploration along the arc, as partly mentioned in Table-1. Precaution has been taken in interpreting the upper-crust brittle deformation as it is intertwined with locally magmatism/ volcanism-related deformation. In addition, we aimed for the discrimination of brittle deformation fabric, marked by tectonic faulting from volcanism-related morphological features, such as radial drainage pattern, lineament of lava flow, sector collapse, or radial and circular fracture.

The location of volcanic features is partly based on Global Volcanism Program, Smithsonian Institution (https://volcano.si.edu/). However, this catalogue only contains large polygenetic volcanic complexes and lacks a considerable number of volcanic features, such as parasitic cones, or monogenetic domes. Therefore, any topographic appearances resembling volcanism, such as circular features, radial pattern, cone and dome are then registered as Quaternary volcanic centres (Figure-2A, 6A, 6B, 7A, 7B, 8A, 8B, and 8C), and then taken into consideration in the structural analysis.

3.2. Distribution and orientation of the basement structures

Previous authors have suggested the existence of series of WNW-ESE structures which determined the depocentres of Eocene-Oligocene sedimentary basins (*Moulds, 1989; Pulunggono, 1992; Hutchison, 1993; Zahirovic et al., 2014*), and yet no one has tried to examine the continuation of WNW-ESE structural series toward the Sumatran Arc, beyond the Tertiary basins. Regional topographic lineaments, the distribution of Pre-Tertiary rock units, and alignment of Quaternary volcanic centres along the Barisan Mountains indicate the continuation of inherited basement structures. They clearly appear along the arc (Figure-2A), and continuously underlie the sedimentary basin as shown by the gravity anomalies (Figure-2B). Along the arc they retain their main orientation of WNW-ESE, although few minor orientations are also observed such as E-W, NNW-SSE, and NW-SE which is somewhat sub-parallel with the SFS. Figure-3 highlights the inherited basement structures along the Barisan Mountains and their spatial relationship with the SFS. While the basement structures have a mostly consistent orientation, some segments of SFS deviate from the general NW-SE to WNW-ESE trend, sub-parallel to the basement structures, notably in the southern segments (Figure-3). Either intersection in acute angle or sub-parallelism between the basement structures and segments of SFS each have created their own particular deformation style.

3.3. Tectonic restoration of Sumatra

Here, we propose to use the Medial Sumatra Tectonic Zone (MSTZ), a suture separating Sibumasu and West Sumatra Terrane (*Barber and Crow, 2003*) (Figure-1A and 1C), as a regional offset marker for the lateral movement along several fault segments in Sumatra, and subsequently restore the strike-slip deformation.

In Toba Caldera Complex, the MSTZ enters the eastern side of SFS in the south, to be displaced by as far as 195 km, and subsequently reappears in the north at the western side of the fault. Farther north again the MSTZ is being displaced by the NNW-SSE dextral Lokop-Kutacane Fault (LKF) for about 60 km (Figure-4). The NW continuation of MSTZ beyond Samalanga Fault is unknown as it may be covered the Tertiary sediment (*Barber and Crow, 2005*).

The LKF which adjoins the north-east side of SFS noticeably has a similar NNW-SSE orientation as the nearby Batee Fault (BF), which adjoins at the south western side of the SFS. The distance between those two adjoining points in the SFS is about 180 km, of the same order of magnitude as the right-lateral displacement of the MSTZ by the SFS to the west of Toba Caldera. This suggests that the LKF and BF once formed one continuous NNW-SSE oriented structure that subsequently was intersected and right-laterally displaced by the younger SFS. This is in accordance with the 65 km offset of two West Sumatra fore-arc basins by BF (*Beaudry and Moore, 1985, in Barber and Crow, 2005*).

The displacement of MSTZ, LKF and BF zone of 190 km, obtained from structural restoration is well in agreement with independent estimates of SFS horizontal displacement. Considering the latest slip-rate for the dextral SFS of 15-16 mm/year (*Bradley et al., 2017; Natawidjaja et al., 2017*) and initiation of the fault in Middle Miocene (±13 Ma) (*McCarthy and Elders, 1997; Barber and Crow, 2005*) leads to an estimate of 190 km total offset, equal to the distance between LKF and BF and in the same range as the amount of MSTZ displacement in the west of Toba Caldera (Figure-3).

Long before the onset of the SFS, the NNW-SSE dextral structural complex was already active and displaced the MSTZ about 55 km northward from its original position (Figure-3A). This NNW-SSE structural grain was the continuation of Late Cretaceous-Paleogene Ranong Fault and Khlong-Marui Fault of peninsular Malaya (*Morley, 2016; Sautter et al., 2017*)

(Figure-1A). It has been manifested as Rayeu Hinge, a basement high separating the Lhok Sukon Deep in the west from the Malaka Platform in the eastern half of North Sumatra Basin (NSB) (*Lunt, 2019*). It possibly acted also as a transfer fault, accommodating the more intense compressional deformation in northern Sumatra, attributed to the shallower subduction slab beneath northern Sumatra. It started around Late Oligocene as indicated by local unconformities in western part of NSB introduced by pop-up transpressional structures (*Lunt, 2019*), supporting previous interpretation by Karig et al (*1980*).

Subsequently, the SFS which initiated in Middle Miocene (13 Ma) (Figure-3B) has displaced the MSTZ and the NNW-SSE structural complex. Since then, the more intense deformation in the northern part has been accommodated by transpressional deformation along SFS.

4. Interaction of the basement structures and the Sumatra Fault System (SFS)

This chapter discusses interactions between the older basement structures and the segments of SFS. The intertwining of two structural features in accommodating the transform component of an oblique subduction system forms fault segmentation and irregularities, and subsequent transtensional and transpressional deformation which also intermingling with volcanism.

4.1. Segmentation of the Sumatra Fault System

The SFS is highly discontinuous, irregular and segmented. This is supported by partitioning of the seismicity along the SFS into earthquake clusters which indicates 16 fault segments (*Burton and Hall, 2014*), and slightly different from the 19 segments interpreted from surface geology by Sieh and Natawidjaja (*2000*). The irregularities in both ends of each fault segment are all located in the intersection between the SFS strands and the basement structures (Figure-3). Therefore, it is proposed that the highly segmented nature of the SFS is the consequence of the intersection and interaction between the younger fault system and a series of pre-existing basement structures. The segmentations and their irregularities along SFS then subsequently lead to local transtensional and transpressional deformations (Figure-6, 7, and 8).

4.2. Transtensional deformation

Along the SFS seventeen intra-arc transtensional pull-apart basins are identified (Figure-3, 6, 7, 8). Table-1 summarizes the main geometrical features of these basins. The best constrained features are the locations of the master or sidewall faults, while intra-basinal structures and basin depths are least constrained. Because the basins maybe partly are hidden under the volcanic covers, i.e. thick ignimbrite layers, multiple lava lobes, and blocks from sector collapses of nearby volcanic flank, the size of the basin (Table-1) is a minimum value. Moreover, the surface topography within the basin is rarely flat, filled-up by alluvial deposits, similar to non-volcanic basins. The lava lobes, volcanic toreva blocks, and surge deposits which frequently flowed and filled in some parts or the entire basins commonly formed hilly and undulating topography within the basin outlines (Figure-6, 7, and 8).

Associated to a dextral strike-slip system, the transtensional deformations along Sumatran Arc are presumably originated from right-stepping of two adjacent fault segments, or in some cases, the releasing bend of a deflected segment. We apply the continuum of basin geometrical development proposed by Mann et al. (*1983*) and Mann (*2007*) (Figure-5A) to classify the shape of the intra-arc basins. Note however that this classification is less suited for depicting irregularities of the basins, such as extreme elongation, non-parallel master faults, tapering toward one end (thus getting wider toward the other), and duplexes and/or anastomosing basins.

More than half of the basins have a length-to-width ratio (L/W) much larger than 3 (Table-1), a typical value for pull-apart basin as suggested by Aydin and Nur (*1982*). It means that the majority of the basins have a highly stretched or elongated geometry.

One type of transtensional deformation style is represented by the Kepahiang (5), Bukit Daun (6), and Hululais (7) basins (Figure-6A). Those basins have an elongated rhomboidal shape with parallel master faults, so that their transverse limit or basinal width is relatively constant throughout its longitudinal axis. Their master faults overlap extensively, and are orientated parallel to regional principal displacement zone (PDZ) trend.

A second distinctive transtensional deformation style is displayed by Sungai Penuh (8), Muara Labuh (9), and Gunung Talang (10) (Figure-6B). Those basins have a more irregular geometry, with a spindle to lazy-Z basin outline. Non parallel master faults of Sungai Penuh (8) generate a pull-apart basin which is tapering off toward its NW end. Its SW master fault is parallel with regional PDZ trend, but the NE master fault slightly swerves from the regional trend. Muara Labuh (9) seemingly has a similar shape, but actually consists of two parts: a main wider part in SE, constructed by parallel fault segments which also swerve from the regional trend, and an elongated narrow tail in the NW. Similarly, the spindle-shape of Gunung Talang (10) is also constructed by parallel master faults which deflect from the regional PDZ trend.

Figure-6C conceptualizes those two distinct transtensional deformation styles along Sumatran Arc. It hypothesizes that the transtensional deformation style is determined by the intersection angle between the segment of SFS and the nearby pre-existing basement structures. The first style, elongated pull-apart basins with parallel master faults and constant width along its longitudinal axis takes place where the basement structures are parallel or sub-parallel with the segments of SFS. The second style, more complex and irregular shaped pull-apart basins develops where the segment of SFS intersects the basement structures in an acute angle. This acute intersection angle allows the nearest segments of intersected basement structures to be reactivated accommodating the slip as oblique strike-slip. As a result, those particular reactivated segments seem to swerve or deflect from regional PDZ trend. Subsequently, it leads to the obliquity of relative movement of the associated block, diverges from regional PDZ trend. Analogue modelling (*Wu et al., 2009*) demonstrates that those two contrasting kinematic settings produce pull-apart basins with a different geometry; the first deformation style produces simpler basin, while the second one generates wider basins with more complex intra-basinal structures, in agreement with the observation in Sumatran Arc.

Furthermore, extensive master faults overlapping in the first deformation style, as in Kepahiang (5), Bukit Daun (6), and Hululais (7) (Figure-6A) are less likely to develop a cross-basinal fault (Figure-5B). This latter feature tends to have developed in the wider pull-apart basins with less overlap of its master faults, as might be the case for the second transtensional deformation style basins in Sungai Penuh (8), Muara Labuh (9), and Gunung Talang (10) (Figure-6B). With the advancement of basin evolution due to progressing fault propagation, this cross-basinal fault eventually is bypassing the displacement along the master faults and basin sidewall faults, connecting the two master faults in order to straighten the fault segment toward regional PDZ trend, and finally terminating the pull-apart basin (*van Wijk et al., 2017; Nabavi et al., 2018*). Therefore, elongated rhomboidal basins with extensive overlapping of master faults tend to have relatively longer lifespan, compared to the wider basins with spindle or lazy-Z shape.

Smaller basins, such as Tarutung (16, Figure-7A), and Ulubelu (1), Natarang (2), Suoh (3) (Figure-7B), might represent the early development stage of intra-arc pull-apart basin. Another elongated basin, Sarulla (15, Figure-7B), seems to be constructed by several small adjoining basins in an anastomosing arrangement if it is in early development stage, or in a duplex setting if it is in an advanced development stage. These adjoining basins are located in the point where MSTZ enters SFS, thus the associated WNW-ESE basement structures are more intense and weak enough to be reactivated as master faults for each sub-basin.

The Rao (13) and Panyabungan Graben (14) (Figure-8B) seem to have a more extensional dip-slip component, as those two basins are closely related and in high-angle to a larger restraining band. Those two basins will be described and discussed more detail in the next chapter.

4.3. Transpressional deformation

Transpressional deformation structures along the Sumatran Arc are briefly summarized in Table-2. The fundamental similarity between these intra-arc transpressional zones is the obvious control of pre-existing WNW-ESE basement structures (Figure-8) in deflecting the SFS segments. All zones are reactivated-segments of basement structures, accommodating the strike-slip displacement of SFS. Uplifts within the wide transpressional zones or narrow restraining bends have been expressed as topographic highs. Subsequent erosion of the highs caused exposure of the Pre-Tertiary basements and/ or Tertiary rock units which then locally were covered by a thin veneer of Quaternary volcanics. Both the lateral extension and elevation of the transpressional zones signals the intensity of the compressional component of deformation. Note that the average and maximum elevation in Table-2 exclude high topography of local volcanic features, and thus represent tectonic uplift rather than volcanism-related positive topography.

It deserves to note that besides WNW-ESE oriented basement structures, NNW-SSE structural grain also controls the two northern transpressional zones: Aceh and Equatorial Bifurcation (EB). NNW-SSE oriented Lokop-Kutacane Fault (LKF) and Batee Fault (BF) seem to enclose NE and SW edges of Aceh transpressional zone (Figure-8A). Similarly, EB is bounded by the NNW-SSE oriented Rao and Panyabungan Graben (Figure-8B). The NNW-SSE orientation of Rao Graben is again intriguingly parallel with Lake Maninjau (MNJ in Figure-8B), an elongated volcanic caldera in further south which is seemingly detached from the surrounding structural trends. As discussed in Chapter 3.3 this NNW-SSE structural trend is continuation of Late Cretaceous-Paleogene regional faults of Peninsular Malaya (Figure-1A) which had been formed during the crustal thickening of Western Sundaland in the Tertiary incurred by northward movement of India (*Sautter et al., 2019*). This trend is more prominent in the northern Sumatra and becomes less obvious toward south. The southernmost transpression, Semendo restraining bend, does not show any trace of NNW-SSE structural trend.

Northern Sumatra

The transpressional zones become smaller from north to the south (Figure-8). The northernmost zone in Aceh (Figure-8A) is the largest and most intense transpressional area, characterized by a vast area of non-volcanic elevated topography. The topography is formed by uplifted Pre-Tertiary basements (Figure-2A) through a series of oblique-reverse faults which form WNW-ESE ridges with an average elevation of 1000 masl and a maximum elevation of more than 3000 masl. Lake Laut Tawar (LT in Figure-8A) is a local depression, presumably piggy-backing on transpressional uplifts. Particular segments in the middle of the zone (red lines in Figure-8A) seem to have the largest strike-slip component compared to the other series of oblique-reverse structures within the zone. These segments therefore accommodated most of the dextral movement of SFS. As previously illustrated in Figure-4A, this region had experienced compressional deformation since Late Oligocene, prior to the onset of SFS. The transpressional zone thus dominates the Northern Sumatra tectono-volcanic domain (TVD), as will be discussed in more detail in the next chapter.

Central Sumatra

Initially, the Equatorial Bifurcation (EB) in Central Sumatra was described as a branching of the SFS into two divergences fault strands which then converge back to eventually form a broad sigmoidal shape in plan-view (*Sieh and Natawidjaja, 2000; Genrich et al., 2000; Natawidjaja, 2017*). Barber and Crow (*2005*) explained this sigmoidal fault bifurcation as a transtensional zones within a releasing step-over. Another interpretation has been proposed by Sahara et al. (*2018*) who suggested a strike-slip duplex system. This paper proposes EB as a transpressional zone, as shown in Figure-8B. Sets of WNW-ESE basement structures around the Medial Sumatra Tectonic zone (MSTZ) form regional weak zones which are reactivated as reverse faults with strike-slip component to accommodates the strike-slip displacement of SFS. In the NW-end of EB, the SFS splits into an eastern oblique reverse fault and a western elongated depression. Subsequently, the two branches of SFS converges back in its SE-end of EB, now oppositely as western oblique reverse fault and eastern elongated depression (Figure-8B). Those elongated topographic depressions, the Rao and Panyabungan Graben (13 and 14 respectively in Table-1) mark the eastern and western margin. A strain ellipsoid analysis on the orientation of depressions and maximum horizontal stress direction (*Mount and Suppe, 1992; Sagala et al., 2018*) suggests that the Rao and Panyabungan Graben have a more extensional component.

Compared to the other two transpressional deformation zones in northern and southern Sumatra, the Equatorial Bifurcation zone has the least elevated topography.

Southern Sumatra

Semendo is the smallest transpressional zone with respect to its lateral extent, yet it has the highest average elevation indicating the concentration of uplift within a small/ narrow area. Compared to the previous two wide transpressional zones which are constructed by series of oblique-reverse faults, Semendo (Figure-8C) is a restraining bend associated with a positive flower-structure (Figure-9).

4.4. Gravity gliding associated with a restraining bend

The presence of an arcuate fold-thrust belt, the Muara Enim anticlinorium, in the distal front of the Semendo restraining bend (Figure-8C) hints to the possibility of a genetic relationship between those two geologic features. The Muara Enim anticlinorium is an arcuate series of asymmetric anticlines alternating with thrusts (Figure-9A) (*Pulunggono, 1986*). The folds are steeply overturned towards the NE, while their arcuate axes concavity faces the Semendo area in SW. Pulunggono (*1986*) had interpreted this anticlinorium as gravitational slumping of Tertiary sediments from the nearby upliftedGumai Mountain basement ridge. However, the location of the uplifted basement in Gumai Mountain is offset from the arcuate anticlinorium rather than directly facing it (Figure-8C and 9B). Therefore, the gravitational slumping is doubly related with the uplifted Gumai Mountain.

Many authors have proposed a genetic association between magmatism-volcanism processes and nearby thin-skinned shortening structures, either due to volcanic loading, magmatic lateral pushing, flank collapsing, or combination of those mechanism (*Merle and Vendeville, 1995; de Vries et al., 2001; Marques and Cobbold, 2002*). However, for the case of the Semendo restraining bend volcanism and associated magmatism seem to contribute little to nothing to the gravitational sliding and associated thin-skinned shortening in its distal area. The Semendo restraining bend builds a prominent topographic high (Table-2) as an accumulation of regional uplifted basements, positive flower-structures, and on top the Quaternary volcanism. Geothermal exploration wells in the NE-flank of the Semendo restraining bend have intersected relatively thin Quaternary volcanic sequences underlain by Tertiary volcanic and sediment strata (*White and Dyaksa, 2015*), which is uncommon for proximal part of a large volcanic complex where thick Quaternary volcanic piles are expected. The occurrence of Tertiary sediments underlying the Quaternary volcanics also supports the general hypothesis that prior to the Barisan Orogeny sedimentation was widespread and connecting Bengkulu Basin and South Sumatra Basin (Figure-9A).

The arcuate Muara Enim anticlinorium is reinterpreted in this paper to be triggered by regional failure and collapse of the flank of Semendo restraining bend due to continuing topographic build-up mostly by positive flower-structures and accumulation of syn-tectonic volcanic products. The block then glided gravitationally north-eastward on top of weak substratum, possibly consisting of shales of the Gumai Fm. as initially suggested by Pulunggono (*1986*), which acts as a decollement surface. The gliding motion directed normal to the general orientation of the restraining bend, then subsequently deformed Tertiary strata in front, thus forming the arcuate asymmetric and overturned thrust-fold belt (Figure-8C, 9A, and 9B). Shallow extensional structures occurred in the gliding block, especially in the side of the Semendo restraining bend and less gradual towards the thrust-fold belt. Those extensional structures partly controlled later lava flows and volcanic domes around Semendo volcanic complexes. Moreover, the alignment of volcanic domes perpendicular to the restraining bend (Figure-8C) can be interpreted as distal parasitic volcanism along the NE-SW transfer faults which accommodated the north-eastward gravitational slump (Figure-9B).

5. Discussions and interpretations

5.1. Brittle deformation and magmatism-volcanism

The spatial correlation between the Quaternary volcanic centres and the dextral SFS along the Sumatran Arc suggests that those two tectonic features are closely associated and reciprocally influence each other. McCarthy and Elders (*1997*) suggested that at a regional scale thermal crustal weakening has concentrated the shear strain of SFS near the volcanic arc. At smaller scale, Bellier and Sebrier (*1994*) and Muraoka et al. (*2010*) genetically correlated some transtensional features along SFS with nearby volcanic centres and/ or calderas. In contrast, Sieh and Natawidjaja (*2000*) and Acocella et al. (*2018*) argue for a weak relationship between magmatism-volcanism and transcurrent deformation along Sumatran Arc. According to them, the close spatial affinity between the segments of the SFS and the volcanic centres is merely coincident and not necessarily related. The offset between the volcanic centres and the segments of the SFS is their main argument to be critical on a possible genetic relationship between those two geological features (*Sieh and Natawidjaja, 2000; Acocella et al., 2018*). However, they only considered prominent and active volcanoes, and did not include smaller volcanic centres, thus their statistical analysis is incomplete and their conclusion less firm.

Besides the Quaternary volcanic centres and the SFS, series of inherited basement structures are proposed in this paper as a new/ additional component in the tectonic evolution of the Sumatran Arc. Figure-2, 6, 7, and 8 show that the location of volcanic centres that are offset from segments of the SFS instead correlate with the basement structures. The basement structures should therefore be considered together with the SFS when expressing and explaining wide band of shear strain and brittle deformation zones present on Sumatra.

Subduction-related magmas are accumulated in a multi-level manner, vertically connected by complex network of diapirs, dykes, and chambers (*Cashman and Sparks, 2013; Cao et al.,* *2016; Magee et al., 2018*). The magmatic arc itself thus should be conceptualized as a broad tectono-volcanic active zone rather than a simple straight line of volcanoes. Accordingly, the linkage between brittle deformation and magmatism in the Sumatra active plate margin could not be assessed from merely fault segments and the alignment of volcanic centres at the surface. A crustal-scale linkage between brittle deformation and magmatism is indicated by the presence of a wide band of shear strain, which in the case of Sumatra consists of the SFS and basement structures, also includes the magmatic intra-lithosphere accumulations in the overriding plate.

The distance between trench and the magmatic arc is mainly determined by the dip of the slab (*Furukawa, 1993; Stern, 2002; Syracuse et al., 2006*), and is not linked to the overriding plate. The accumulated melt subsequently migrates upward through upper mantle and lower crust driven by buoyancy. The upper part of the magmatic plumbing system eventually requires permeable pathways in the overlying brittle crust to facilitate further upward movement of magma. Both the basement structures and active segments of younger faults potentially provide favourable pathways where pulses of magma could propagate to shallower levels or even reach the surface. However, because the basement structures are older and longer in place, they may have contributed more to the ascent of magma by providing more permeable pathways.

Following the ascent of magmas, elevated temperatures around those magmatic bodies reduces the brittle yield strength of the crustal rocks. This thermal weakening promotes further brittle deformation and concentrating of strain (*Cao and Neubauer, 2016*). Such a positive feedback between magmatic emplacement and brittle deformation can be postulated for the Sumatran case study. Figure-10 conceptualizes this interplay, where the basement structures control not only the SFS's irregularity, but also the ascent of magma and the volcanic lineament.

The cooling plutons beneath an inactive volcanic complex are still hot enough to continue weaken the crust, and thereby to facilitate reactivation of basement structures also in volcanic inactive regions away from the SFS.

5.2. Origin of the inherited basement structures

The orientation of the basement structures is broadly homogeneous over the whole length of the arc, and is dominantly WNW-ESE as demonstrated by the rose-diagrams in Figure-3. This consistent orientation is intriguing considering that Sumatra has experienced repeated subductions and subsequent tectonic fragment amalgamations from early Mesozoic to present day. It might be explained by the fact that those phases of subduction and amalgamation had a roughly similar tectonic orientation, as interpreted from the general orientation of tectonic blocks and sutures which all run broadly parallel to the long axis of the island (Figure-1A). It may therefore be likely that older basement structures formed from previous tectonic events were not significantly modified by the later tectonic phases/ events. The currently observed basement structures are thus a cumulative product of the long history of convergences in Sumatra.

Another explanation might be that the inherited basement structures were formed mainly by the last major tectonic event, which was the accretion of Woyla Terrane to Sumatra in the Late Cretaceous. The slight change in the orientation of basement structures i.e., to be NW-SE in the southernmost segment of arc (Figure-3, and 7B) might be attributed to the internal heterogeneities within Woyla Block itself, considering its complex nature as a remnant itself of a string of oceanic island arc segments. Figure-12 illustrates the arrangement of basement structures in multiple tectonic blocks, and also highlights the contribution of basement structures to the strike-slip deformation and volcanism along the arc, and the sedimentary basin configuration farther away from the arc.

5.3. Division of the Sumatran Arc

At present time, the Sumatran Arc is dominated by both the active Neogene SFS and the Quaternary volcanic chain. That is why we primarily use the variation of spatial relationships between the SFS and the volcanic arc as an initial basis for dividing the Sumatran Arc into three main tectono-volcanic domains (TVD) (Figure-11 and 12). As discussed in the previous chapters, the way the SFS acts in accommodating the transform component of oblique subduction, either as purely strike-slip, transtensional, or transpressional deformation, is mainly determined by pre-existing heterogeneities within the overriding plate, i.e. the basement structures. The active volcanic arc is instead largely determined by lateral variations of the subducting plate, i.e. the dip of the slab (Figure-11), as a commonly the case for subduction-related volcanic arc.

Whereas in the southern and central TVD the Quaternary volcanic centres are roughly located along the main strand of the SFS, these are shifted apart in the northern TVD. This contrasting spatial relationship exists without significant crustal-scale differences between the southern and northern overriding plate (*Pasyanos et al., 2014; Yu et al., 2017*). The inherited basement structures also have a broadly similar orientation in all TVDs (Figure-4). Therefore, we attribute the contrast between in particular the southern and northern TVD to the heterogeneities of the incoming plate and subducted slab beneath Sumatra.

The subducting slab below the Southern TVD is older (>60 Ma), thus denser and heavier, and subsequently lead to a steeper subduction dip and narrower trench-volcanic gap. Conversely, the subducting slab beneath the Northern TVD is younger, hotter, and partly composed of the remnants of inactive spreading centres (*Malod and Kemal, 1996; Jacob et al., 2014*). This more buoyant slab leads to a gentler subduction dip angle and a larger trench-volcanic gap i.e., volcanism is further inland, away from the trench. Malod and Kemal (*1996*) suggest that younger subducting oceanic lithosphere and its inactive spreading centres may also lead to a stronger coupling between the slab and the overriding plate. This stronger coupling also exerts additional stresses which cause buckling and flexural bulging in the oceanic side of the trench in Northern TVD (*Raghuram et al., 2018*). This strong coupling, paired with the possibility of slightly more rigid overriding plate attributed to the arc assemblage of Woyla Block (*Cameron et al., 1980*), may explain the more intensive deformation in form of wide transpressional zone, expressed as broader and higher topographic high in Northern TVD. The vast volcanic region of the Toba caldera with its extensive rhyolitic volcaniclastic and resurgent volcanism (*Chesner, 2012; Westgate et al, 2013; Costa et al., 2014*) marks the transition zone between those two distinctive volcano-tectonic domains.

The contrasting volcano-tectonic characteristic of Northern and Southern TVD, and also the distinctive magmatism in the transitional Central domain, are all primarily influenced by the subducting slab (Figure-11 and 12), with the overriding plate only plays minor role. The division of Sumatran Arc into three TVD broadly resembles structural domains previously proposed by Sieh and Natawidjaja (*2000*). However, these structural domains are mainly attributed to the evolution of intra-arc deformation and the influence of trench-parallel extension in the fore-arc sliver, which has been revised by a latter study. Instead of assuming extensional deformation, Bradley et al. (*2017*) have proposed a rigid fore-arc sliver and similar slip rate along the SFS. Previously, a more complex SFS structural setting around the equator, such as the Equatorial Bifurcation (*Sieh and Natawidjaja, 2000; Weller et al., 2012; Natawidjaja, 2018*) was considered to be a result of internal deformation of the fore-arc sliver, and consequently was included in the Central domain (*Sieh and Natawidjaja, 2000*). In this paper we argue that the Equatorial Bifurcation is a transpressional zone controlled by a specific interaction between the SFS and WNW-ESE basement structures, and possibly also a less obvious NNW-SSE structural trend, we therefore propose to consider the Equatorial Bifurcation deformation zone to be part of Southern TVD.

6. Conclusions

The paper presents a study of the interaction between pre-existing basement structures, the younger strike-slip fault, and the occurrence of individual volcanic centres. Regular patterns of the Palaeozoic-Mesozoic basements generally have a WNW-ESE to a more limited NW-SE orientation. The structural relationship between the younger dextral strike-slip Sumatra Fault System (SFS) and the basement structures can be observed along the entire length of the Sumatran Arc. Geometrical irregularity, segmentation and deflections of the SFS's strands, the complex structure of intra-arc pull-apart basins, transpressional zones and restraining bends are all primarily determined by the interaction with the inherited/ pre-existing basement structures. This relation has often been recognised locally or inferred in other arcs system or transcurrent fault zone, but to our knowledge at such a scale and with the clarity the Sumatran Arc provides one of the best example.

Two transtensional deformation styles are present, differing in and controlled by the intersection angle between the SFS and the basement structures. Where the segments of SFS are parallel or sub-parallel to the basement structures, elongated rhomboidal pull-apart basins develop with parallel and extensively overlapping master faults, and thus with a constant width along their longitudinal axis. When the intersection angle between the SFS and the basement structures is larger, pull-apart basins develop with a more irregular geometry, ranging from spindle to a lazy-Z shape.

Transpressional zones occur on Sumatra where the basement structures are reactivated as series of reverse faults to accommodate the first-order transform deformation. A wider and more intense transpressional zone in the northern Sumatra is probably caused by a stronger coupling between the subducting and overriding plate. The transpressional zones get smaller southward and manifest as a narrow yet intense restraining bend in Semendo (southern Sumatra). There local intense uplift triggered gravitational slumping which subsequently deformed Tertiary sediments in the distal part of the Semendo restraining bend.

Quaternary volcanoes and the SFS are concentrated in a relatively narrow zone over the length of the arc, suggesting a positive correlation. However, besides a few exceptions, the volcanoes are not localised on the fault strands or in one of the numerous pull-apart basins along the SFS. Instead, volcanoes are located along the inherited basement structures, sometimes with several volcanoes along the same inherited structures. An interplay and positive feedback between intra-crust syn-tectonic magmatism and brittle deformation is proposed as possible explanation of close spatial relationship between the basement structures, the irregularity of the SFS, and the volcanic centres.

Lastly, the Sumatran Arc can be divided into three domains based on their tectono-volcanic aspects. Those three distinctive tectono-volcanic characteristics are mainly determined by the nature of subducting plate, rather than heterogeneities within the overriding plate.

References

Acocella, V., et al. (2018). "Weak tectono-magmatic relationships along an obliquely convergent plate boundary: Sumatra, Indonesia." Frontiers in Earth Science 6: 3.

Advokaat, E. L., et al. (2018). "Early Cretaceous origin of the Woyla Arc (Sumatra, Indonesia) on the Australian plate." Earth and Planetary Science Letters 498: 348-361.

Advokaat, E. L., et al. (2018). "Cenozoic rotation history of Borneo and Sundaland, SE Asia revealed by paleomagnetism, seismic tomography, and kinematic reconstruction." Tectonics 37(8): 2486-2512.

Aldiss, D. and S. Ghazali (1984). "The regional geology and evolution of the Toba volcano-tectonic depression, Indonesia." Journal of the Geological Society 141(3): 487-500.

Aribowo, S. (2018). The geometry of pull-apart basins in the southern part of Sumatran strike-slip fault zone. IOP Conf. Ser. Earth Environ. Sci.

Aydin, A. and A. Nur (1982). "Evolution of pull-apart basins and their scale independence." Tectonics 1(1): 91-105.

Barber, A. (2000). "The origin of the Woyla Terranes in Sumatra and the Late Mesozoic evolution of the Sundaland margin." Journal of Asian Earth Sciences 18(6): 713-738.

Barber, A. and M. Crow (2005). "Structure and structural history." Geological Society, London, Memoirs 31(1): 175-233.

Barber, A., et al. (2005). "Tectonic evolution." Geological Society, London, Memoirs 31(1): 234-259.

Barber, A., et al. (2005). "Introduction and previous research." Geological Society, London, Memoirs 31(1): 1-6.

Barber, A. J. and M. J. Crow (2003). "An Evaluation of Plate Tectonic Models for the Development of Sumatra." Gondwana Research 6(1): 1-28.

Barber, A. J. and M. J. Crow (2009). "Structure of Sumatra and its implications for the tectonic assembly of Southeast Asia and the destruction of Paleotethys." Island Arc 18(1): 3-20.

Beaudry, D. and G. F. Moore (1985). "Seismic stratigraphy and Cenozoic evolution of West Sumatra forearc basin." AAPG bulletin 69(5): 742-759.

Bellier, O. and M. Sébrier (1994). "Relationship between tectonism and volcanism along the Great Sumatran fault zone deduced by SPOT image analyses." Tectonophysics 233(3-4): 215-231.

Bradley, K. E., et al. (2017). "Implications of the diffuse deformation of the Indian Ocean lithosphere for slip partitioning of oblique plate convergence in Sumatra." Journal of Geophysical Research: Solid Earth 122(1): 572-591.

Burton, P. W. and T. R. Hall (2014). "Segmentation of the Sumatran fault." Geophysical Research Letters 41(12): 4149-4158.

Cameron, N. R., et al. (1980). "The Geological Evolution of Northern Sumatra." Indonesian Petroleum Association 9th Annual Convention Proceedings: 149-187.

Cao, S. and F. Neubauer (2016). "Deep crustal expressions of exhumed strike-slip fault systems: Shear zone initiation on rheological boundaries." Earth-Science Reviews 162: 155-176.

Cao, W., et al. (2016). "Intrusion of granitic magma into the continental crust facilitated by magma pulsing and dike-diapir interactions: Numerical simulations." Tectonics 35(6): 1575-1594.

Cashman, K. V. and R. S. J. Sparks (2013). "How volcanoes work: A 25 year perspective." GSA bulletin 125(5-6): 664-690.

Chemenda, A., et al. (2000). "Strain partitioning and interplate friction in oblique subduction zones: Constraints provided by experimental modeling." Journal of Geophysical Research: Solid Earth 105(B3): 5567-5581.

Chesner, C. A. (2012). "The Toba caldera complex." Quaternary International 258: 5-18.

Chlieh, M., et al. (2008). "Heterogeneous coupling of the Sumatran megathrust constrained by geodetic and paleogeodetic measurements." Journal of Geophysical Research: Solid Earth 113(B5).

Cloetingh, S. and R. Wortel (1986). "Stress in the Indo-Australian plate." Tectonophysics 132(1-3): 49-67.

Costa, A., et al. (2014). "The magnitude and impact of the Youngest Toba Tuff super-eruption." Frontiers in Earth Science 2: 16.

Crow, M. J. and A. J. Barber (2005). "Map: Simplified geological map of Sumatra." Geological Society, London, Memoirs 31(1): NP-NP.

Curray, J., et al. (1979). "Tectonics of the Andaman Sea and Burma: convergent margins." M 29: Geological and Geophysical Investigations of Continental Margins: 189-198.

Daud, Y., et al. (2000). Integrated geophysical studies of the Ulubelu geothermal field, south Sumatera, Indonesia. Proceedings World geothermal congress.

Davies, P. R. (1984). "Tertiary structural evolution and related hydrocarbon occurrences, North Sumatra Basin." Indonesian Petroleum Association 13th Annual Convention Proceedings (Volume 1): 19-49.

DeMets, C., et al. (2010). "Geologically current plate motions." Geophysical Journal International 181(1): 1-80.

De Vries, B. V. W., et al. (2001). "A gravitational spreading origin for the Socompa debris avalanche." Journal of Volcanology and Geothermal Research 105(3): 225-247.

Dir. Panas Bumi dan PSDMBPB. (2017). "Potensi Panas Bumi Indonesia." Dir.Panas Bumi, Dirjen. EBTKE, KESDM.

Eubank, R. T. and A. C. Makki (1981). "Structural geology of the Central Sumatra back-arc basin." Indonesian Petroleum Association 10th Annual Convention Proceedings: 153-196.

Fauzi, et al. (1996). "Lateral variation in slab orientation beneath Toba Caldera, northern Sumatra." Geophysical Research Letters 23(5): 443-446.

Fernandez-Blanco, D., et al. (2016). "Structure and kinematics of the Sumatran fault system in North Sumatra (Indonesia)." Tectonophysics 693: 453-464.

Fontaine, H. and S. Gafoer (1989). "The pre-Tertiary fossils of Sumatra and their environments." CCOP Technical Papers 19. United Nations.

Furukawa, Y. (1993). "Magmatic processes under arcs and formation of the volcanic front." Journal of Geophysical Research: Solid Earth 98(B5): 8309-8319.

Gasparon, M. and R. Varne (1998). "Crustal assimilation versus subducted sediment input in west Sunda arc volcanics: an evaluation." Mineralogy and Petrology 64(1-4): 89-117.

Genrich, J., et al. (2000). "Distribution of slip at the northern Sumatran fault system." Journal of Geophysical Research: Solid Earth 105(B12): 28327-28341.

Global Volcanism Program, 2013. Volcanoes of the World, v. 4.9.1 (17 Sep 2020). Venzke, E (ed.). Smithsonian Institution. https://doi.org/10.5479/si.GVP.VOTW4-2013.

Hall, R. (2002). "Cenozoic geological and plate tectonic evolution of SE Asia and the SW Pacific: computer-based reconstructions, model and animations." Journal of Asian Earth Sciences 20(4): 353-431.

Hall, R. (2012). "Late Jurassic–Cenozoic reconstructions of the Indonesian region and the Indian Ocean." Tectonophysics 570: 1-41.

Hall, R. and C. K. Morley (2004). Sundaland Basins. Continent-Ocean Interactions Within East Asian Marginal Seas: 55-85.

Hall, R. and W. Spakman (2015). "Mantle structure and tectonic history of SE Asia." Tectonophysics 658: 14-45.

Heidrick, T. L. and K. Aulia (1993). "A structural and tectonic model of the coastal plains block, Central Sumatra Basin, Indonesia." Indonesian Petroleum Association 22nd Annual Convention Proceedings (Volume 1): 285-317.

Hickman, R., et al. (2004). "Tectonic and stratigraphic evolution of the Sarulla graben geothermal area, North Sumatra, Indonesia." Journal of Asian Earth Sciences 23(3): 435-448.

Howles Jr, A. (1986). "Structural and stratigraphic evolution of the southwest Sumatran Bengkulu shelf." Indonesian Petroleum Association 15th Annual Convention Proceedings (Volume 1): 215-243.

Huchon, P. and X. Le Pichon (1984). "Sunda Strait and central Sumatra fault." Geology 12(11): 668-672.

Hutchison, C. S. (1994). Gondwana and Cathaysian blocks, Palaeotethys sutures and Cenozoic tectonics in South-east Asia. Active Continental Margins — Present and Past. P. Giese and J. Behrmann. Berlin, Heidelberg, Springer Berlin Heidelberg: 388-405.

Jacob, J., et al. (2014). "Revisiting the structure, age, and evolution of the Wharton Basin to better understand subduction under Indonesia." Journal of Geophysical Research: Solid Earth 119(1): 169-190.

Karig, D., et al. (1980). "Structural frame work of the fore-arc basin, NW Sumatra." Journal of the Geological Society 137(1): 77-91.

Katili, J. A. H., F. (1967). "On the occurrence of Large Transcurrent Faults in Sumatra, Indonesia." J. Geosciences Osaka City Univ 10: 5-17.

Koulakov, I., et al. (2016). "The feeder system of the Toba supervolcano from the slab to the shallow reservoir." Nature communications 7(1): 1-12.

Lange, D., et al. (2010). "The fine structure of the subducted investigator fracture zone in western Sumatra as seen by local seismicity." Earth and Planetary Science Letters 298(1-2): 47-56.

Lunt, P. (2019). "Partitioned transtensional Cenozoic stratigraphic development of North Sumatra." Marine and Petroleum Geology 106: 1-16.

Magee, C., et al. (2018). "Magma plumbing systems: a geophysical perspective." Journal of Petrology 59(6): 1217-1251.

Malod, J. A. and B. M. Kemal (1996). "The Sumatra margin: oblique subduction and lateral displacement of the accretionary prism." Geological Society, London, Special Publications 106(1): 19-28.

Mann, P. (2007). "Global catalogue, classification and tectonic origins of restraining- and releasing bends on active and ancient strike-slip fault systems." Geological Society, London, Special Publications 290(1): 13-142.

Mann, P., et al. (1983). "Development of pull-apart basins." The Journal of Geology 91(5): 529-554.

Marques, F. and P. Cobbold (2002). "Topography as a major factor in the development of arcuate thrust belts: insights from sandbox experiments." Tectonophysics 348(4): 247-268.

McCaffrey, R. (1991). "Slip vectors and stretching of the Sumatran fore arc." Geology 19(9): 881-884.

McCaffrey, R. (2009). "The tectonic framework of the Sumatran subduction zone." Annual Review of Earth and Planetary Sciences 37: 345-366.

McCaffrey, R., et al. (2000). "Strain partitioning during oblique plate convergence in northern Sumatra: Geodetic and seismologic constraints and numerical modeling." Journal of Geophysical Research: Solid Earth 105(B12): 28363-28376.

McCarthy, A. and C. Elders (1997). "Cenozoic deformation in Sumatra: oblique subduction and the development of the Sumatran Fault System." Geological Society, London, Special Publications 126(1): 355-363.

McKenzie, D. and J. G. Sclater (1971). "The evolution of the Indian Ocean since the Late Cretaceous." Geophysical Journal International 24(5): 437-528.

Merle, O. and B. Vendeville (1995). "Experimental modelling of thin-skinned shortening around magmatic intrusions." Bulletin of Volcanology 57(1): 33-43.

Metcalfe, I. (2000). "The Bentong–Raub Suture Zone." Journal of Asian Earth Sciences 18(6): 691-712.

Metcalfe, I. (2011). "Tectonic framework and Phanerozoic evolution of Sundaland." Gondwana Research 19(1): 3-21.

Morley, C. (2016). "Cenozoic structural evolution of the Andaman Sea: evolution from an extensional to a sheared margin." Geological Society, London, Special Publications 431(1): 39-61.

Moulds, P. (1989). "Development of the Bengkalis depression, central Sumatra and its subsequent deformation–A model for other Sumatran Grabens?" Indonesian Petroleum Association 18th Annual Convention Proceedings (Volume 1), 1989: 217-245.

Mount, V. S. and J. Suppe (1992). "Present-day stress orientations adjacent to active strike-slip faults: California and Sumatra." Journal of Geophysical Research: Solid Earth 97(B8): 11995-12013.

Mukti, M. (2018). "Structural configuration and depositional history of the Semangko pull-apart basin in the southeastern segment of Sumatra Fault Zone." Riset Geologi dan Pertambangan Vol. 28, No.1: 115-128.

Muraoka, H., et al. (2010). Geothermal systems constrained by the Sumatran fault and its pull-apart basins in Sumatra, western Indonesia. Proceedings World Geothermal Congress.

Mussofan, W., et al. (2018). Geothermal resource exploration along Great Sumatera Fault segments in Muara Laboh: perspectives from geology and structural play. Proceedings, 43rd Workshop on Geothermal Reservoir Engineering, Stanford University. SGP-TR-213.

Nabavi, S. T., et al. (2018). "2D finite-element elastic models of transtensional pull-apart basins." Comptes Rendus Geoscience 350(5): 222-230.

Natawidjaja, D. H. (2018). "Major Bifurcations, Slip Rates, and A Creeping Segment of Sumatran Fault Zone in Tarutung-Sarulla-Sipirok-Padangsidempuan, Central Sumatra, Indonesia." Indonesian Journal on Geoscience 5(2): 137-160.

Natawidjaja, D. H., et al. (2017). "Late Quaternary eruption of the Ranau Caldera and new geological slip rates of the Sumatran Fault Zone in Southern Sumatra, Indonesia." Geoscience Letters 4(1): 21.

Niasari, S. W., et al. (2015). 3D inversion of magnetotelluric data from the Sipoholon geothermal field, Sumatra, Indonesia. World Geothermal Congress 2015.

Nishimura, S., et al. (1986). "Neo-tectonics of the Strait of Sunda, Indonesia." Journal of Southeast Asian Earth Sciences 1(2): 81-91.

Nukman, M. and I. Moeck (2013). "Structural controls on a geothermal system in the Tarutung Basin, north central Sumatra." Journal of Asian Earth Sciences 74: 86-96.

Page, B. G. N., et al. (1979). "A review of the main structural and magmatic features of northern Sumatra." Journal of the Geological Society 136(5): 569-577.

Pasyanos, M. E., et al. (2014). "LITHO1. 0: An updated crust and lithospheric model of the Earth." Journal of Geophysical Research: Solid Earth 119(3): 2153-2173.

Pesicek, J., et al. (2008). "Complex slab subduction beneath northern Sumatra." Geophysical Research Letters 35(20).

Posavec, M., et al. (1973). "Tectonic controls of volcanism and complex movements along the Sumatran Fault System." Geol. Soc. Malaysia Bulletin 6: 43-60.

Prawirodirdjo, L., et al. (1997). "Geodetic observations of interseismic strain segmentation at the Sumatra subduction zone." Geophysical Research Letters 24(21): 2601-2604.

Prawirodirdjo, L., et al. (2010). "Geodetic observations of an earthquake cycle at the Sumatra subduction zone: Role of interseismic strain segmentation." Journal of Geophysical Research: Solid Earth 115(B3).

Pubellier, M. and C. Morley (2014). "The basins of Sundaland (SE Asia): Evolution and boundary conditions." Marine and Petroleum Geology 58: 555-578.

Pulunggono, A. (1986). "Tertiary structural features related to extensional and compressive tectonics in the Palembang Basin, South Sumatra." Indonesian Petroleum Association 15th Annual Convention Proceedings (Volume 1): 187-213.

Pulunggono, A. and N. Cameron (1984). "Sumatran microplates, their characteristics and their role in the evolution of the Central and South Sumatra basins." Indonesian Petroleum Association 13th Annual Convention Proceedings (Volume 1): 121-143.

Pulunggono, A., et al. (1992). "Pre-Tertiary and Tertiary Fault Systems as a Framework of the South Sumatra Basin; A Study of SAR-Maps." Indonesian Petroleum Association 21st Annual Convention Proceedings (Volume 1): 339-360.

Raghuram, G., et al. (2018). "Flexural Analysis Along the Sunda Trench: Bending, Buckling and Plate Coupling." Tectonics 37(10): 3524-3544.

Sagala, B. D., et al. (2016). "Conceptual model of Sorik Marapi geothermal system based on 3-G data interpretation." Proceedings of IIGCE 2016.

Sahara, D. P., et al. (2018). "Stress heterogeneity and its impact on seismicity pattern along the equatorial bifurcation zone of the Great Sumatran Fault, Indonesia." Journal of Asian Earth Sciences 164: 1-8.

Sandwell, D. T. and W. H. Smith (1997). "Marine gravity anomaly from Geosat and ERS 1 satellite altimetry." Journal of Geophysical Research: Solid Earth 102(B5): 10039-10054.

Sautter, B., et al. (2017). "Late Paleogene rifting along the Malay Peninsula thickened crust." Tectonophysics 710: 205-224.

Sautter, B., et al. (2019). "Exhumation of west Sundaland: A record of the path of India?" Earth-Science Reviews 198: 102933.

Schütt, J. M. and D. M. Whipp (2020). "Controls on Continental Strain Partitioning Above an Oblique Subduction Zone, Northern Andes." Tectonics 39(4): e2019TC005886.

Seymour, N. M., et al. (2020). "The Relationship Between Magmatism and Deformation Along the Intra-arc Strike-Slip Atacama Fault System, Northern Chile." Tectonics 39(3): e2019TC005702.

Sieh, K. and D. Natawidjaja (2000). "Neotectonics of the Sumatran fault, Indonesia." Journal of Geophysical Research: Solid Earth 105(B12): 28295-28326.

Simandjuntak, T. and A. Barber (1996). "Contrasting tectonic styles in the Neogene orogenic belts of Indonesia." Geological Society, London, Special Publications 106(1): 185-201.

Stern, R. J. (2002). "Subduction zones." Reviews of geophysics 40(4): 3-1-3-38.

Syracuse, E. M. and G. A. Abers (2006). "Global compilation of variations in slab depth beneath arc volcanoes and implications." Geochemistry, Geophysics, Geosystems 7(5).

Van Wijk, J., et al. (2017). "Initiation, evolution and extinction of pull-apart basins: Implications for opening of the Gulf of California." Tectonophysics 719: 37-50.

Weller, O., et al. (2012). "The structure of the Sumatran Fault revealed by local seismicity." Geophysical Research Letters 39(1).

Westgate, J., et al. (2013). "Tephrochronology of the Toba tuffs: four primary glass populations define the 75-ka Youngest Toba Tuff, northern Sumatra, Indonesia." Journal of Quaternary Science 28(8): 772-776.

White, P. and D. Dyaksa (2015). Relic and modern epidote: lessons from Rantau Dedap, Sumatra. Proceedings 37th New Zealand Geothermal Workshop.

Williams, H. H. and R. T. Eubank (1995). "Hydrocarbon habitat in the rift graben of the Central Sumatra Basin, Indonesia." Geological Society, London, Special Publications 80(1): 331-371.

Wu, J. E., et al. (2009). "4D analogue modelling of transtensional pull-apart basins." Marine and Petroleum Geology 26(8): 1608-1623.

Yu, C., et al. (2017). "Deep thermal structure of Southeast Asia constrained by S-velocity data." Marine Geophysical Research 38(4): 341-355.

Zahirovic, S., et al. (2014). "The cretaceous and cenozoic tectonic evolution of Southeast Asia." Solid Earth 5(1): 227-273.

Acknowledgements

This work was conducted as part of the Geothermal Capacity Building programme Indonesia – the Netherlands (GEOCAP). LS is funded by the Indonesian Endowment Fund for Education (LPDP) and by the GEOCAP programme.

Data Availability Statement

The regional digital elevation model used for the morphological observation and interpretation is extracted from the 0.27 arc-second resolution National Indonesia DEM (*http://tides.big.go.id/DEMNAS*). Regional gravimetry is from Sandwell and Smith (2009); while seismicity is from USGS earthquake catalogue (*https://www.usgs.gov/ natural-hazards/earthquake-hazards/lists-maps-and-statistics*).

Figures and Tables

Table-1. Summary of Sumatran intra-arc pull-apart basin

Table-2. Summary of Sumatran transpressional zones

Figure-1. **(A)** Tectonic framework of Sumatra as part of the western half of Sundaland. **(B)** Regional structures of the incoming Indo-Australian Plate and contour map (in km) of its subducted slab, reinterpreted from global P-wave velocity anomaly model UU-P07 (*Hall and Spakman, 2015*). **(C)** NE-SW conceptual cross-section across Sumatra, modified from *Barber et al. (2005)*; location is shown in Fig. 1-A. Microplates and sutures are modified from *Barber et al. (2005)* and *Metcalfe (2011, 2013)*; in alphabetical order: *BRZ*: Bentong-Raub Zone, *EMB*: East Malaya Block, *MSTZ*: Medial Sumatra Tectonic Zone, *SIB*: Sibumasu Block, *WBB*: West Burma Block, *WOY*: Woyla Block, *WSB*: West Sumatra Block. Regional structures are modified from *Morley (2015)*, *Berglar et al. (2010, 2017)*, and *Sautter et al. (2017, 2019)*, in alphabetical order: *BF*: Batee Fault, *KMF*: Khlong-Marui Fault, *MF*: Mentawai Fault, *RF*: Ranong Fault, *SB*: Siberut Fault, *SFS*: Sumatran Fault System, *SS*: Sunda Strait, *TPF*: Three-Pagodas Fault. Quaternary volcanic centers are from *Smithsonian Institution Global Volcanism Program (volcano.si.edu)*. Convergence vectors are from MORVEL (*DeMets et al., 2010*). Structures of the incoming Indo-Australian Plate are from *Jacob et al. (2014)*. Some focal mechanisms are selected from Global CMT catalogue (*www.globalcmt.org*) for contrasting deformation in the fore-arc and along the SFS.

Figure-2. (A) Regional geologic map of Sumatran Arc i.e., Barisan Mountains modified from *Crow and Barber (2005)*. It shows exposed Paleozoic-Mesozoic rocks, covered by Tertiary and Quaternary volcanics. The fore-arc structures are modified from *Sieh and Natawidjaja (2000)* and *Berglar et al. (2010)*. **(B)** Regional gravity field of Sumatra and the surrounding area overlain by basement structures along the arc (black straight lines) and its continuation toward the back-arc region (white dashed lines). The free-air gravity is from *Sandwell and Smith (2009)*.

Figure-3. Orientation of the inherited basement structures (black) compared to the traces of SFS (red). Numbers identify the intra-arc basins (dark blue, refer to Table-1), and squares with alphabet are location of more detail maps in Figure-8. Shaded grey is elevated topography of the arc, light blue patches are lakes. Colour in the rose diagrams follows the maps.

Figure-4. Restoration of SFS based on the offset of MSTZ (dark blue band). **(A)** In Late Oligocene (±25 Ma) the NNW-SSE major structure started to be active and eventually shifted MSTZ northward. This structure was manifested as a hinge line separated the Western (darker grey) from yet to be formed Eastern basinal area (lighter grey) in NSB. Notes the occurrence of basement structures which partly controlled the outline of basin depocentres (darker grey). **(B)** Middle Miocene (±13 Ma) was the onset of dextral movement of SFS, simultaneous with the uplift of Barisan Mountains; sedimentary basin was then separated into back-arc and more limited extend fore-arc basins, and syn-orogenic sedimentary facies succeeded previous transgressive sequence. Yellow marks the would-be contractional area caused by later transpressional deformation. The NNW-SSE structures was reactivated as LKF and BF. **(C)** Present time when MSTZ, LKF, and BF have been displaced around 190km. Notes that the southern segments of MSTZ are largely covered by Tertiary sediments. Greyscale shows depth of the basement. *NSB*: North Sumatra Basin, *CSB*: Central Sumatra Basin, *SSB*: South

Sumatra Basin. Orange lines in (B) and (C) demonstrate the dextral displacement of basement structure.

Figure-5. **(A)** Geometrical types of transtensional zone, redrawn from *Mann (2007)*. (B) Component of a pull-apart basin as reference figure for Table-1.

Figure-6. (A) Elongated rhomboidal intra-arc basins; notes that SFS (red) are almost parallel with the basement structures (black). **(C)** Lazy-Z intra-arc basins where intersection angle between SFS (red) and the basement structures is larger. Refer to text for explanation. Numbers refer to Table-1. Circles are Quaternary volcanic centres; intra-arc basin is shaded blue, while dark blue is lake. **(C)** Conceptual block diagram for two transtensional deformation styles generated by different intersection angle between SFS's segments (red) and the basement structures (black). It is expressed in the geometry of intra-arc pull-apart basin.

Figure-7. **(A)** Small adjoining sub-basins form an elongated pull-apart basin in Sarulla. Note that MSTZ intersects SFS at this basin. **(B)** Southernmost intra-arc basins with spindle to lazy-Z shape. Refer to text for explanation. Map's legend is similar with Figure-6. Numbers refer to Table-1.

Figure-8. Three major transpressional deformations along the arc; **(A)** the northern region/ Aceh, **(B)** Equatorial Bifurcation in the centre, and **(C)** Semendo in the south. Note SW-NE cross-section for Figure-9 in (C). *LT*: Lake Laut Tawar, *PNY*: Panyabungan basin, *RAO*: Rao basin, *MNJ*: Lake Maninjau, *SEM*: Semendo, *ME*: Muara Enim arcuate anticlinorium, *BB*: Bengkulu Basin. Location of the maps are indicated in Figure-4; numbering of intra-arc basin refers to Table-1.

Figure-9. Hypothetical gravitational sliding connects Semendo elevated topography in the SW and arcuate Muara Enim anticlinorium in the NE. **(A)** SW-NE cross-section from

Bengkulu Basin to western South Sumatra Basin; refer to Figure-6C for map view. Bengkulu Basin is modified from *Hall et al. (1993)*, Muara Enim anticlinorium is modified from *Pulunggono (1986)*. *Lt*: Lemat Fm., *Se*: Seblat Fm., *Hu*: Hulusimpang Fm., *Lu*: Lemau Fm., *Ta*: Talangakar Fm., *Gu*: Gumai Fm., *Ab*: Air Benakat Fm., *Me*: Muara Enim Fm., *Mb*: Mesozoic basement, *Ts*: Tertiary sediment, *Qv*: Quaternary volcanics. **(B)** conceptual model of Semendo restraining bend, gravitational sliding, and Muara Enim anticlinorium. High topography is accumulatively produced from the uplifted basement, pop-up of a restraining bend, and volcanism on top.

Figure-10. Postulated conceptual model of an interplay between brittle deformation of the inherited basement structures and younger SFS, and syn-tectonic magmatism/ volcanism. Note the basement structures which control SFS's irregularity, magma ascending, and volcanic lineament. Cooling plutons beneath an inactive volcanic complex are still hot enough to weaken the crust. Refer to text for explanation. *LAB*: lithosphere-asthenosphere boundary, *MASH*: melting, assimilation, storage, homogenization zone.

Figure-11. Heterogeneity of subducted slab beneath Sumatra creates different tectono-volcanic domains (TVD) along Sumatran Arc. For explanation, refer to Figure-1B and the text.

Figure-12. Tectono-volcanism/ magmatism domains (TVD) along Sumatran Arc. Northern TVD **(A)** is dominated by transpressional deformation where the volcanic centres are slightly shifted away from the main strand of SFS, and sit on top of thrusted basement structures. In contrast, Southern TVD **(C)** is where regularly distributed volcanic centres coexist with the SFS, while Central TVD **(B)** is basically the transition zone. Voluminous magmatism/ volcanism of Toba is related to the slab tearing below. Inset conceptualizes various orientation of basement structures with respect to the tectonic blocks, and roles of basement structures farther east in Tertiary sedimentary basin.

Table-1. Summary of Sumatran intra-arc pull-apart basin (*1: Daud et al., 2000; 2: Dir.Panas Bumi dan PSDMBPB, 2017; 3: Mussofan et al., 2018; 4: Sagala et al., 2016; 5: Hickman et al., 2004; 6: Niasari et al., 2015*)

Number *(Fig-4)*	Basin Name	Geometry						Orientation *(N…°E)*		Remarks
		Length (km)	Width (km)	L/W	Area (km^2)	Max depth (m)	Shape *(Mann et al., 1983)*	Master fault	Regional trend	
1	**Ulubelu**	8	7	1,1	55	±500 *(1)*	Spindle	118	124	Lava flows and volcaniclastic form hilly topography inside the basin
2	**Natarang**	6	5	1,2	27	n/a	Spindle	130	136	Terraced basin margin in the SE-part
3	**Suoh**	11	7	1,6	82	2200 *(2)*	Lazy-Z	131	136	-
4	**Ranau**	11	14	0,8	130	n/a	Lazy-Z (?)	130	132	alternative interpretation is a fault-controlled caldera due to peculiar basin shape
5	**Kepahiang**	27	5	5,4	134	n/a	Rhomboidal	134	136	Parallel master faults; lava flows form hilly topography in the NW-part
6	**Bukit Daun**	15	3	5,0	59	n/a	Rhomboidal	140	140	Parallel master faults; volcaniclastics form hilly topography inside the basin
7	**Hululais**	30	6	5,0	203	n/a	Rhomboidal	137	140	Parallel master faults; lava flows form hilly topography in the SE-part
8	**Sungai Penuh**	45	10	4,5	300	n/a	Lazy-Z	136 (NE margin), 148 (SW margin)	148	Non-parallel master faults; tapers off toward NW edge; lava flows form hilly topography in the SE-part
9	**Muara Labuh**	14	10	1,4	147 (SE-part)	2000 *(3)*	Lazy-Z	120	145	Lazy-Z shape in the SE-part, elongated narrow basin in the NW-tail; lava flows and volcaniclastics form hilly topography
10	**Gunung Talang**	7	6	1,2	46	n/a	Spindle	125	150	-
11	**Singkarak**	20	6	3,3	115	n/a	Spindle	140	140	Long axis is parallel with the major trend, NW-edge is slightly widened by deflected segment (N121°E)
12	**Lubuk Sikaping**	15	3	5,0	41	n/a	Spindle	151	149	Parallel master faults; lava flows form hilly topography in the SE-part
13	**Rao Graben**	30	7	4,3	216	n/a	Spindle (?)	163	164	Eastern branch of Equatorial Bifurcation; more distinctive eastern-border fault; extensional component (dip-slip) is more prominent
14	**Panyabungan Graben**	39	7	5,6	321	1500 *(4)*	Spindle (?)	156	157	Western branch of Equatorial Bifurcation, more distinctive western-border fault, extensional component (dip-slip) is more prominent
15	**Sarulla**	37	6	6,2	168	2200 *(5)*	Spindle	147	150	Narrow pull-apart systems; also possible as a duplex or anastomosing pull-apart basins
16	**Tarutung**	7	3	2,3	34	1300 *(6)*	Spindle	138	146	-
17	**Kutacane**	44	10	4,4	304	n/a	Lazy-Z	140	142	Interaction between SFS and LKF; LKF segment controls NW sidewall fault, and SFS segment controls NE and SW master faults

Table-2. Summary of Sumatran transpressional zones (**: excluding volcanic-related topographic high*)

Map *(Fig-8)*	Basin Name	Geometry					Remarks
		Length (km)	Width (km)	Area (km^2)	Average elevation* (masl)	Max elevation* (masl)	
A	**Aceh**	220	150	28000	1070	3200	Wide transpressional zone; controlled by WNW-ESE basement structures and NNW-SSE structural trends
B	**Equatorial Bifurcation**	90	65	4400	800	1800	Transpressional zone controlled by WNW-ESE basement structures and NNW-SSE structural trends; associated with Rao and Panyabungan Graben as its NW and SE margin respectively
C	**Semendo**	67	22	1620	1450	2600	Restraining bend controlled by WNW-ESE basement structures, but NNW-SSE structural trends are absent; create gravitational collapse

Figure-1.

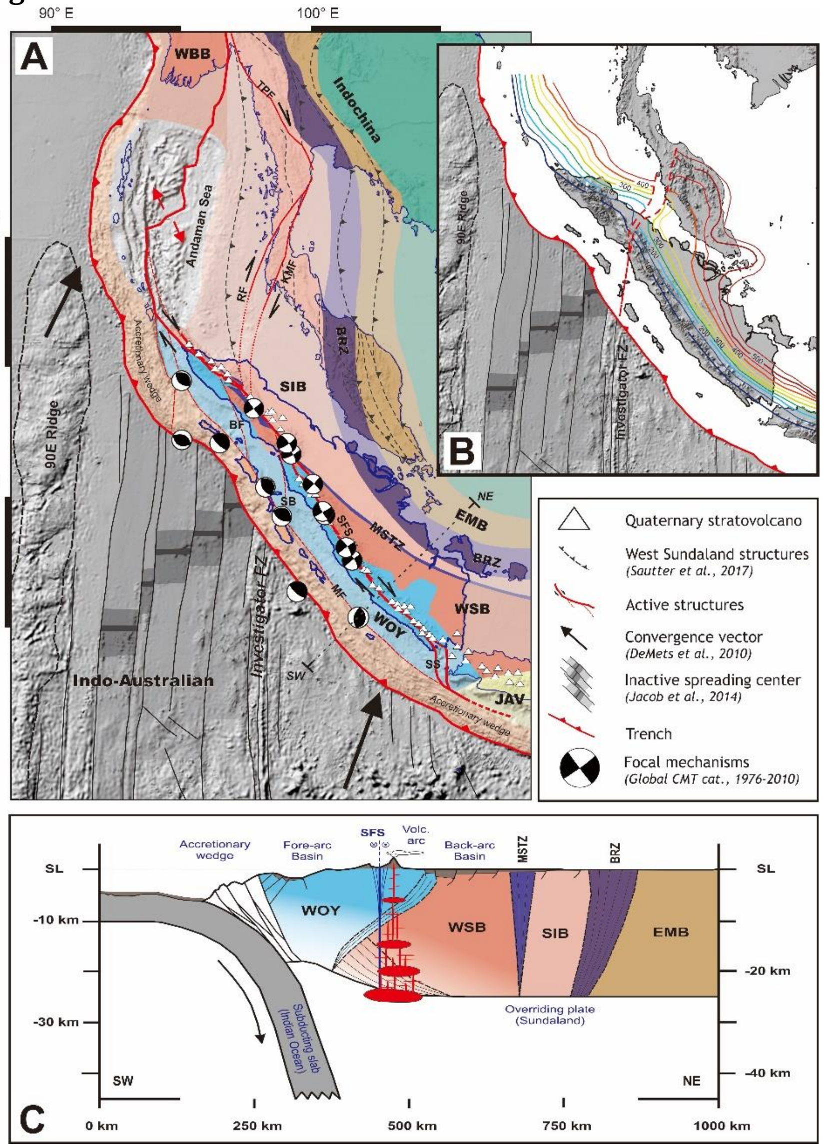

A
B
C
90° E
100° E
10° N
0° N
WBB
Indochina
Andaman Sea
TPF
KMF
RF
BRZ
SIB
BF
SB
SFS
MSTZ
EMB
BRZ
WSB
WOY
MF
SS
JAV
NE
SW
90E Ridge
Indo-Australian
Investigator FZ
Accretionary wedge
Quaternary stratovolcano
West Sundaland structures
(Sautter et al., 2017)
Active structures
Convergence vector
(DeMets et al., 2010)
Inactive spreading center
(Jacob et al., 2014)
Trench
Focal mechanisms
(Global CMT cat., 1976-2010)
Accretionary wodgo
Fore-arc Basin
SFS
Volc. arc
Back-arc Basin
MSTZ
BRZ
SL
-10 km
-20 km
-30 km
-40 km
WOY
WSB
SIB
EMB
Subducting slab (Indian Ocean)
Overriding plate (Sundaland)
SW
NE
0 km
250 km
500 km
750 km
1000 km

Figure-2.

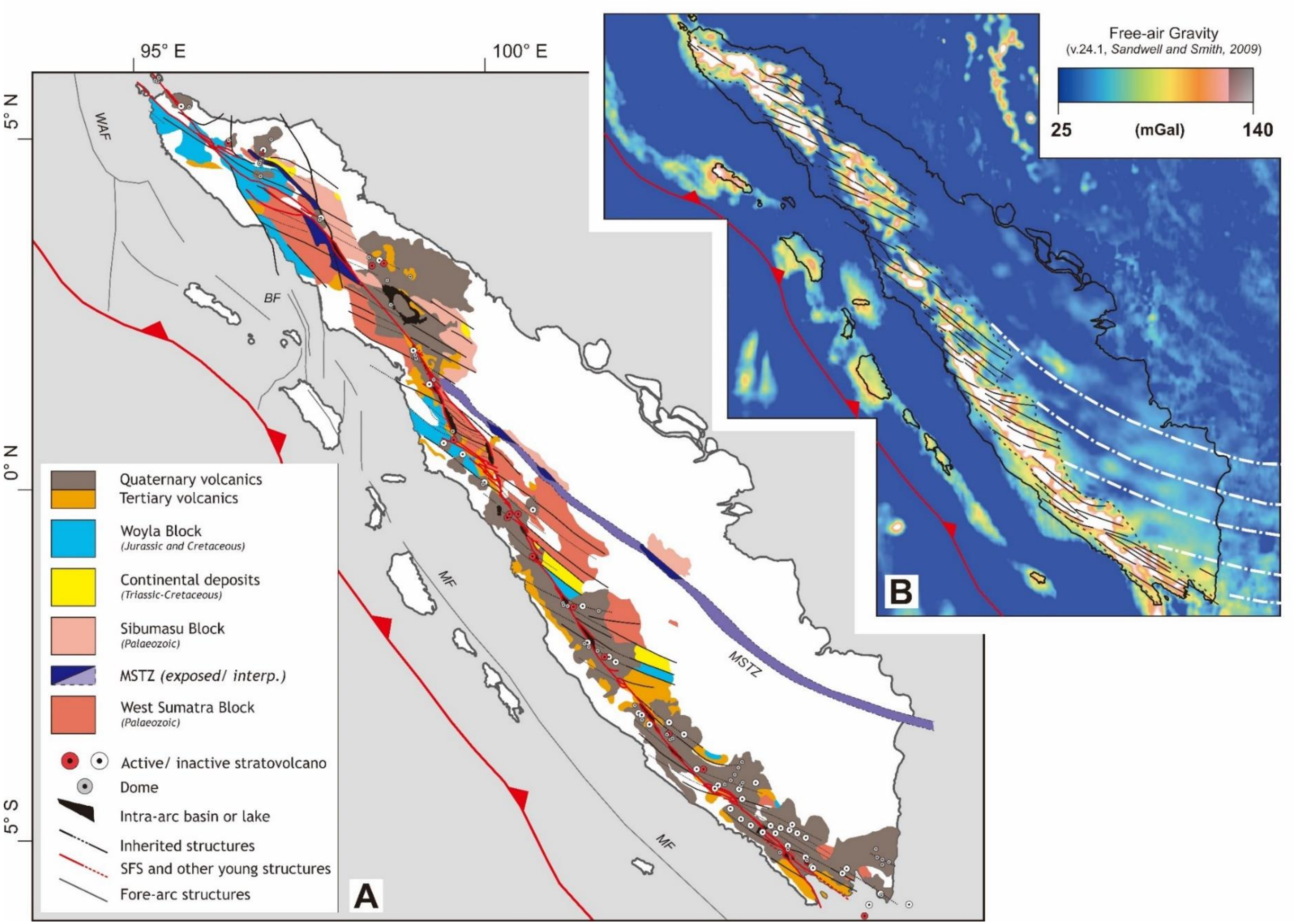
95° E
100° E
5° N
0° N
5° S
WAF
BF
MF
MF
MSTZ
Quaternary volcanics
Tertiary volcanics
Woyla Block
(Jurassic and Cretaceous)
Continental deposits
(Triassic-Cretaceous)
Sibumasu Block
(Palaeozoic)
MSTZ (exposed/ interp.)
West Sumatra Block
(Palaeozoic)
Active/ inactive stratovolcano
Dome
Intra-arc basin or lake
Inherited structures
SFS and other young structures
Fore-arc structures
A
Free-air Gravity
(v.24.1, Sandwell and Smith, 2009)
25
(mGal)
140
B

1096 Figure-3.

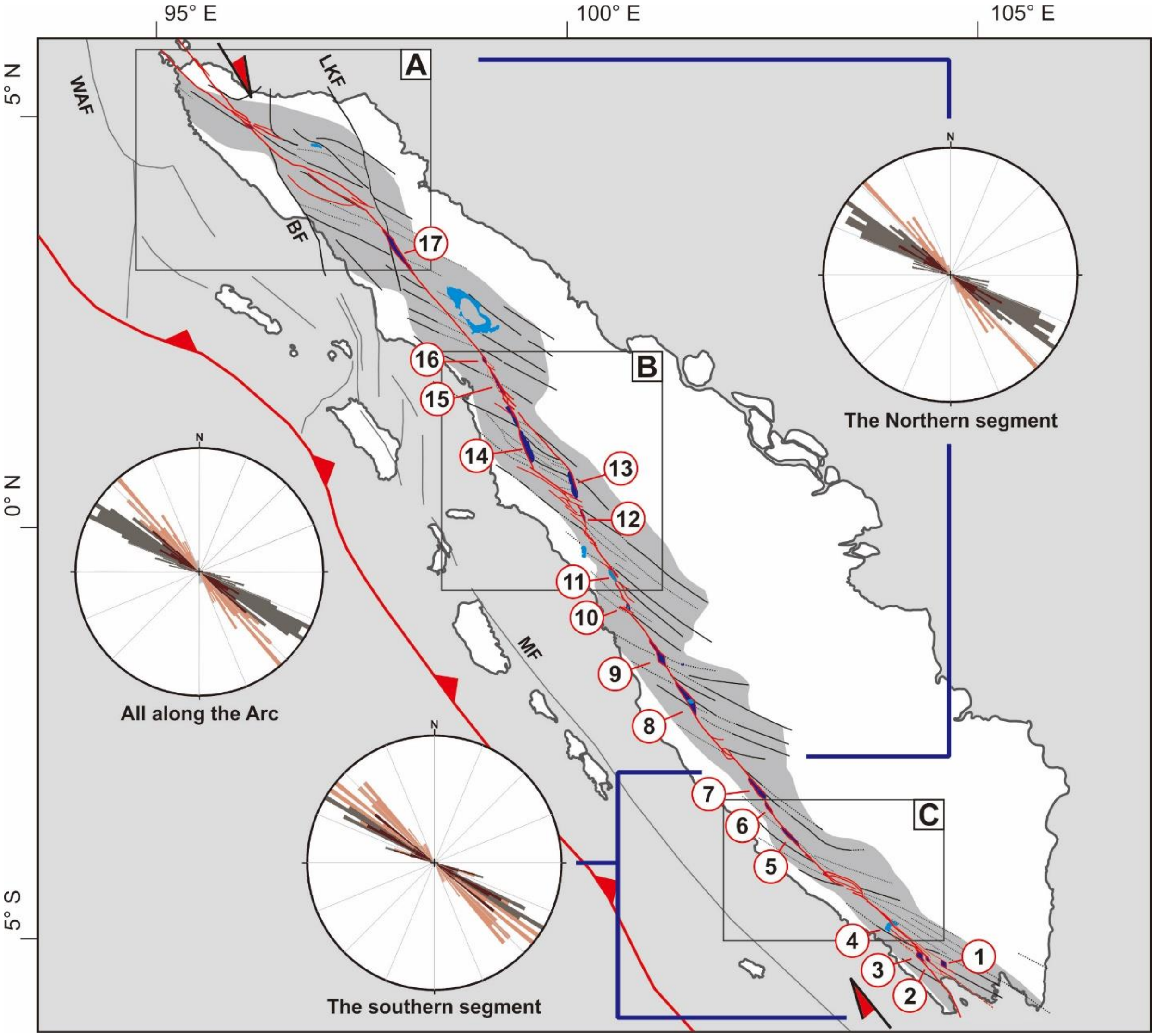

1097

Figure-4.

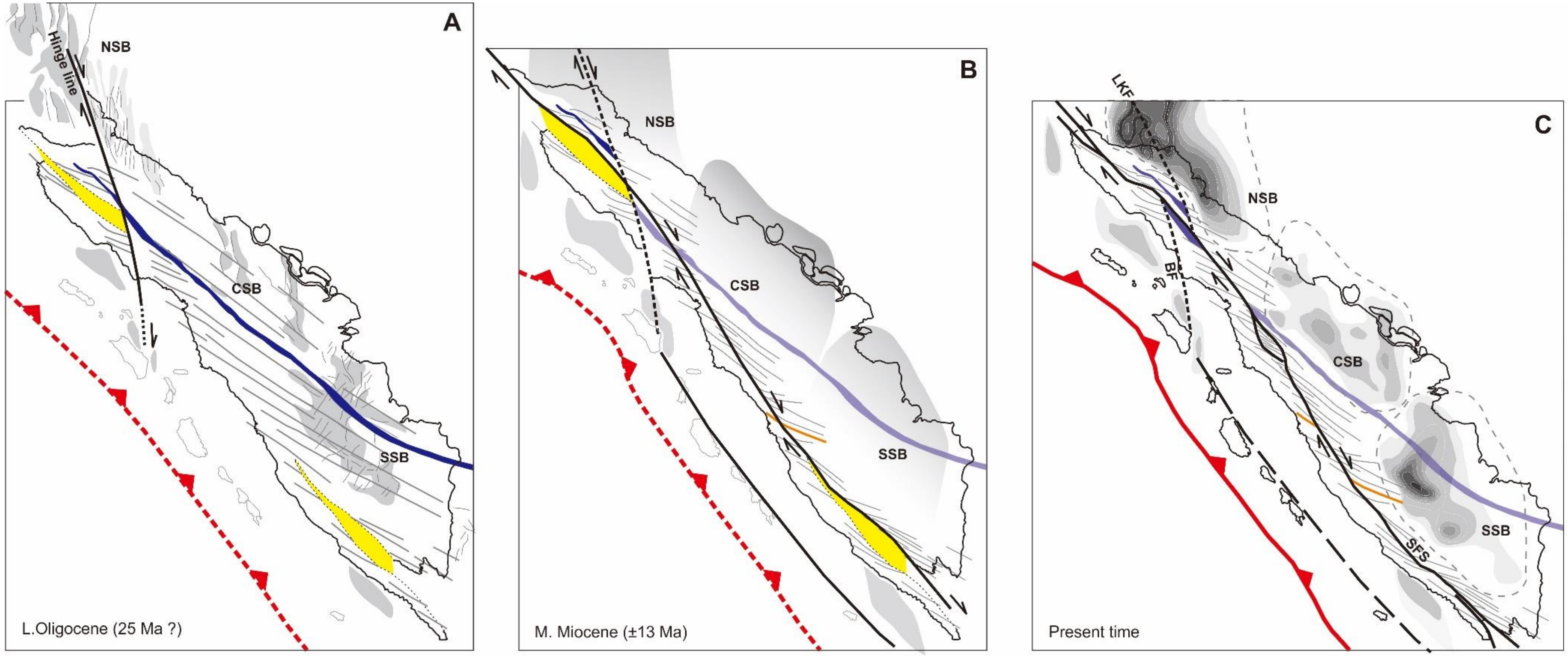
A
Hinge line
NSB
CSB
SSB
L.Oligocene (25 Ma ?)
B
NSB
CSB
SSB
M. Miocene (±13 Ma)
C
LKF
NSB
BF
CSB
SSB
SFS
Present time

Figure-5.

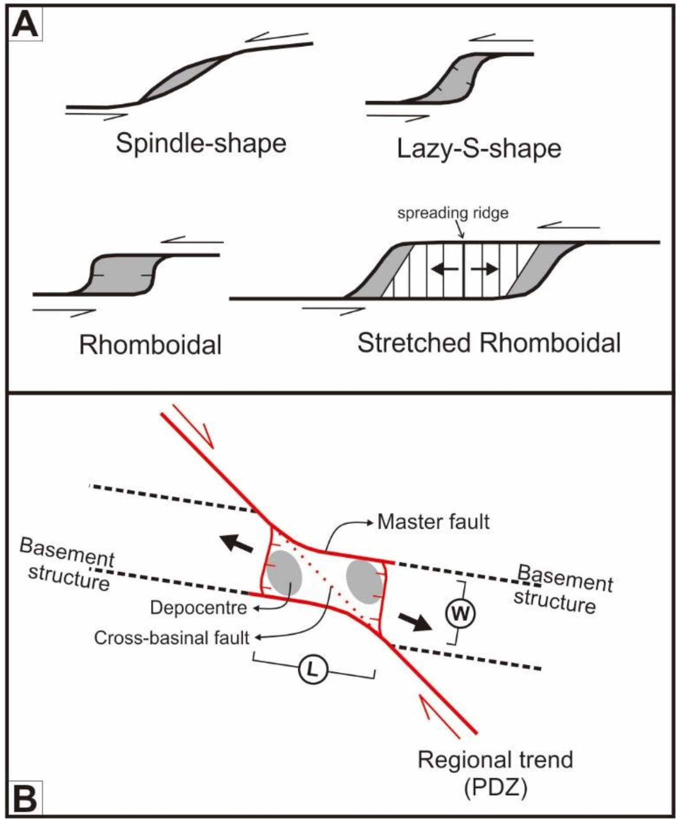
A
Spindle-shape
Lazy-S-shape
spreading ridge
Rhomboidal
Stretched Rhomboidal
Master fault
Basement structure
Basement structure
Depocentre
Cross-basinal fault
W
L
Regional trend (PDZ)
B

Figure-6.

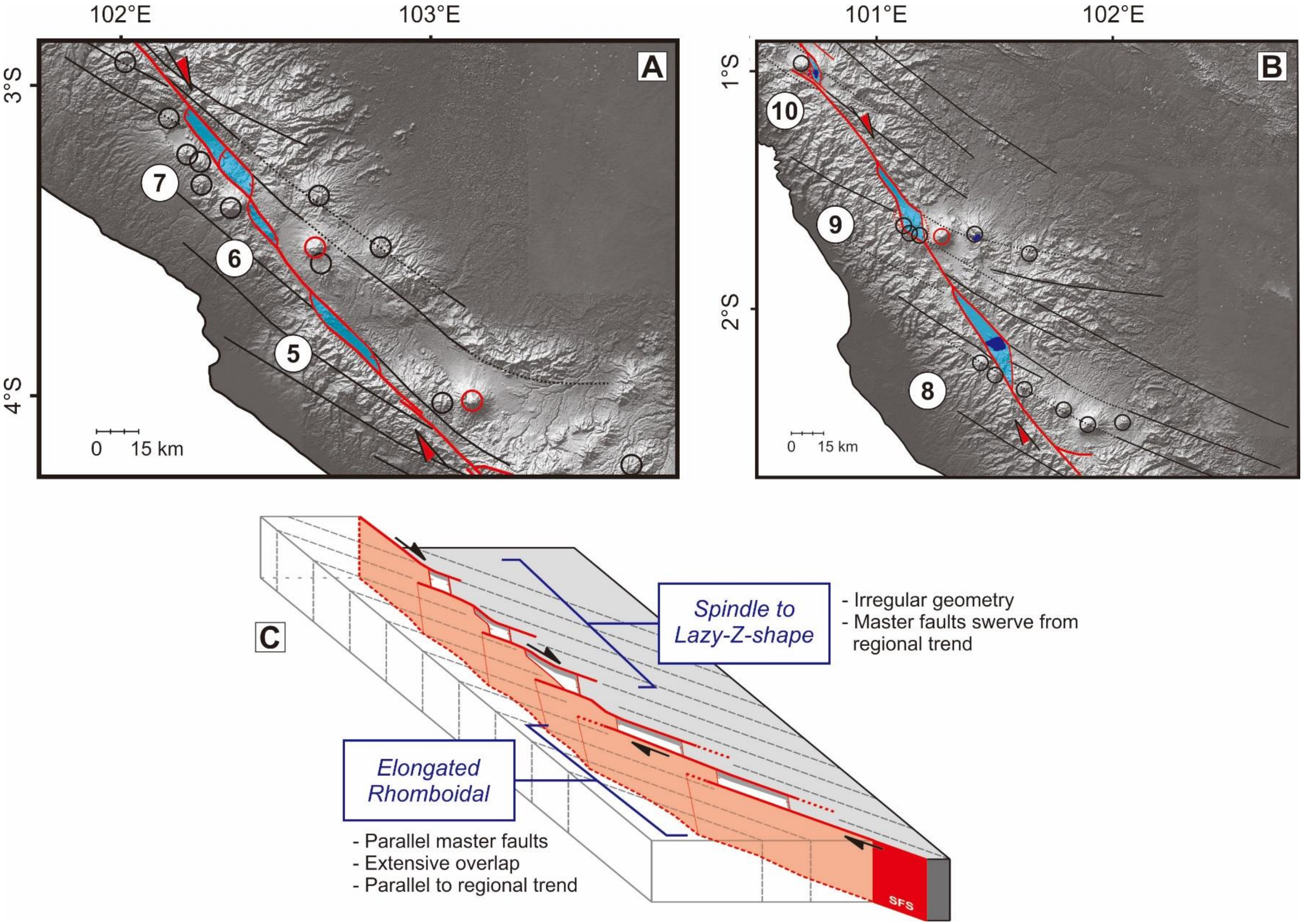

102°E
103°E
3°S
4°S
A
7
6
5
0 15 km
101°E
102°E
1°S
2°S
B
10
9
8
0 15 km
C
Spindle to
Lazy-Z-shape
- Irregular geometry
- Master faults swerve from
regional trend
Elongated
Rhomboidal
- Parallel master faults
- Extensive overlap
- Parallel to regional trend
SFS

Figure-7.

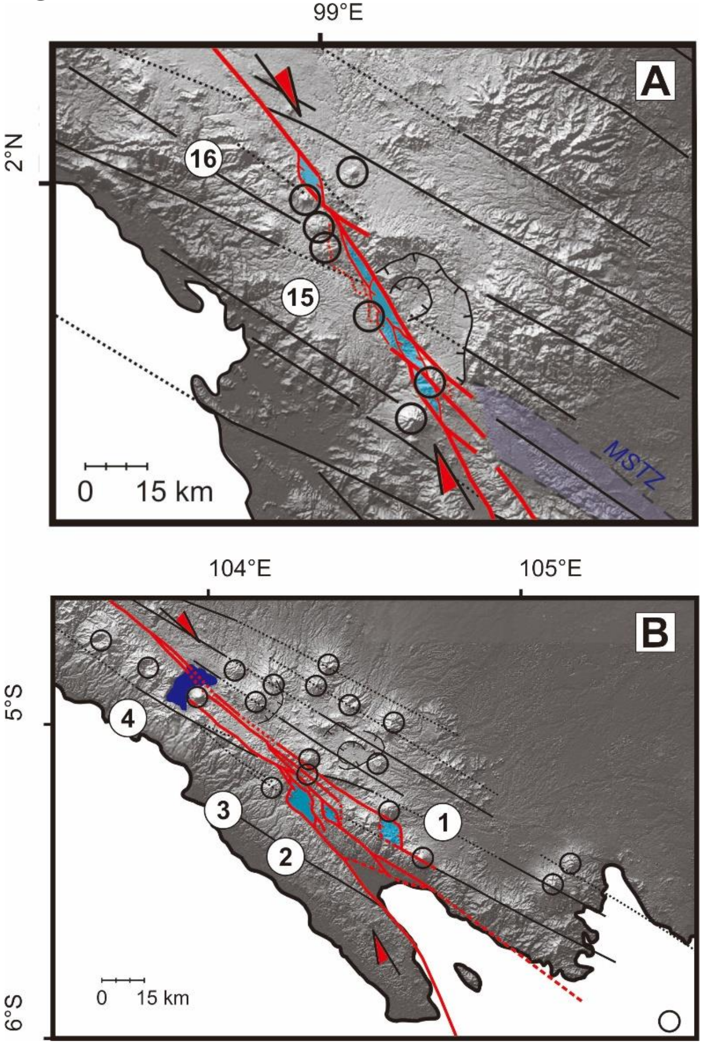

Figure-8.

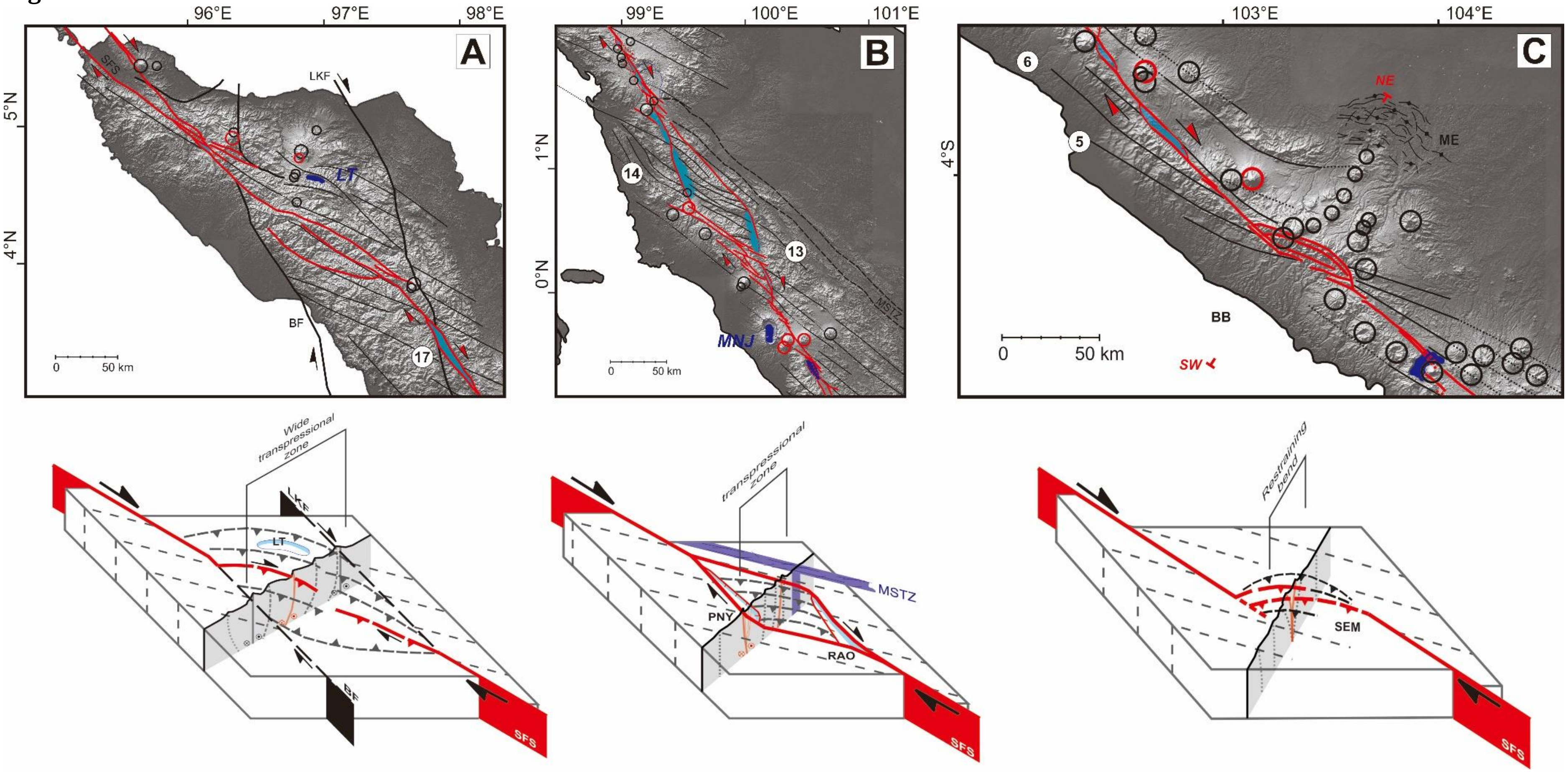
96°E
97°E
98°E
99°E
100°E
101°E
103°E
104°E
5°N
4°N
1°N
0°N
4°S
A
B
C
SFS
LKF
LT
BF
17
0
50 km
14
13
MSTZ
MNJ
6
5
NE
ME
BB
SW
Wide transpressional zone
LKF
LT
BF
SFS
transpressional zone
MSTZ
PNY
RAO
SFS
Restraining bend
SEM
SFS

Figure-9.

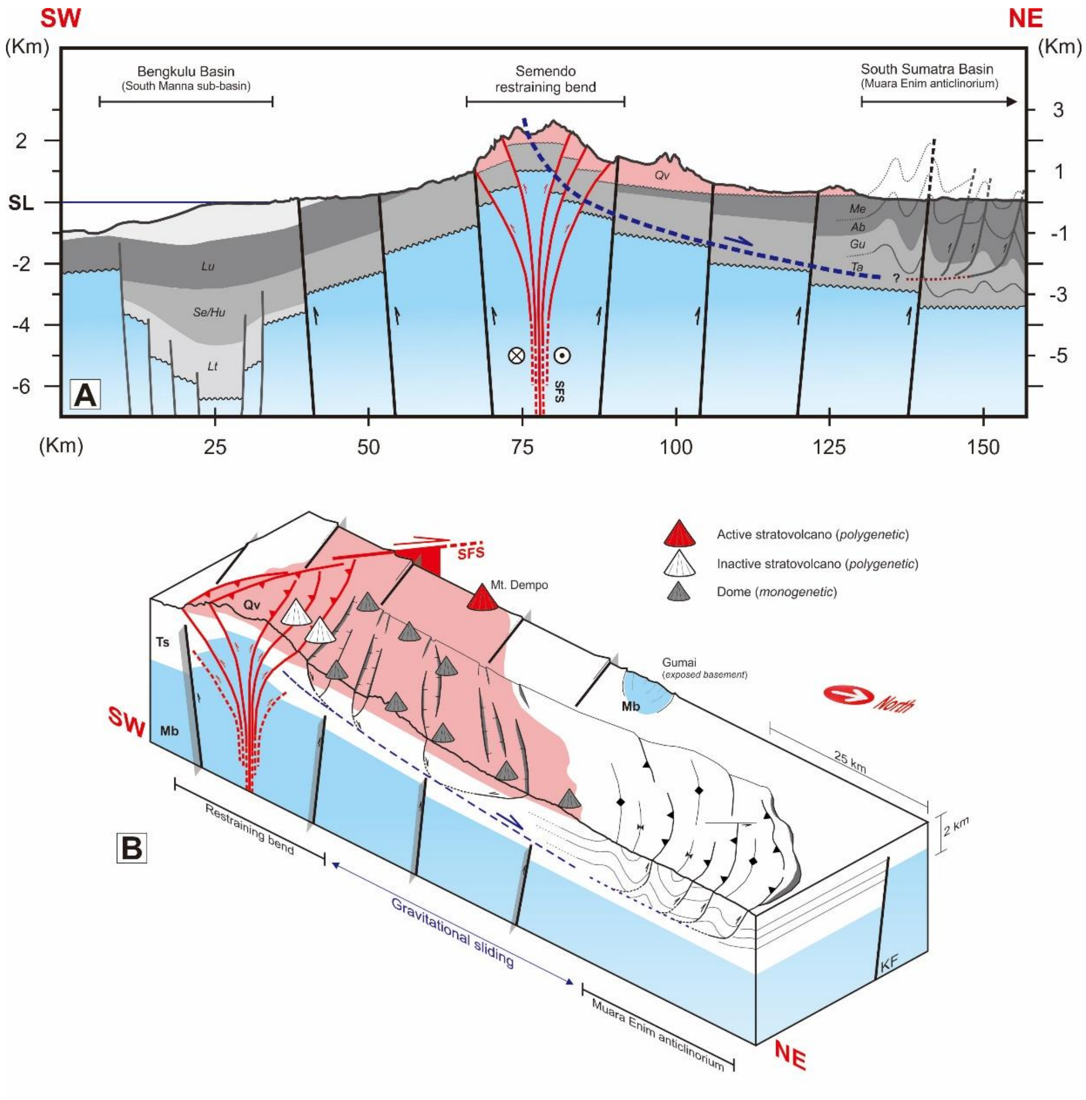

SW
NE
(Km)
Bengkulu Basin
(South Manna sub-basin)
Semendo
restraining bend
South Sumatra Basin
(Muara Enim anticlinorium)
3
2
1
SL
-1
-2
-3
-4
-5
-6
Qv
Me
Ab
Gu
Ta
Lu
Se/Hu
Lt
SFS
A
25
50
75
100
125
150
Active stratovolcano (polygenetic)
Inactive stratovolcano (polygenetic)
Dome (monogenetic)
Mt. Dempo
SFS
Qv
Ts
Mb
Gumai
(exposed basement)
Mb
North
25 km
2 km
Restraining bend
Gravitational sliding
Muara Enim anticlinorium
KF
B

Figure-10.

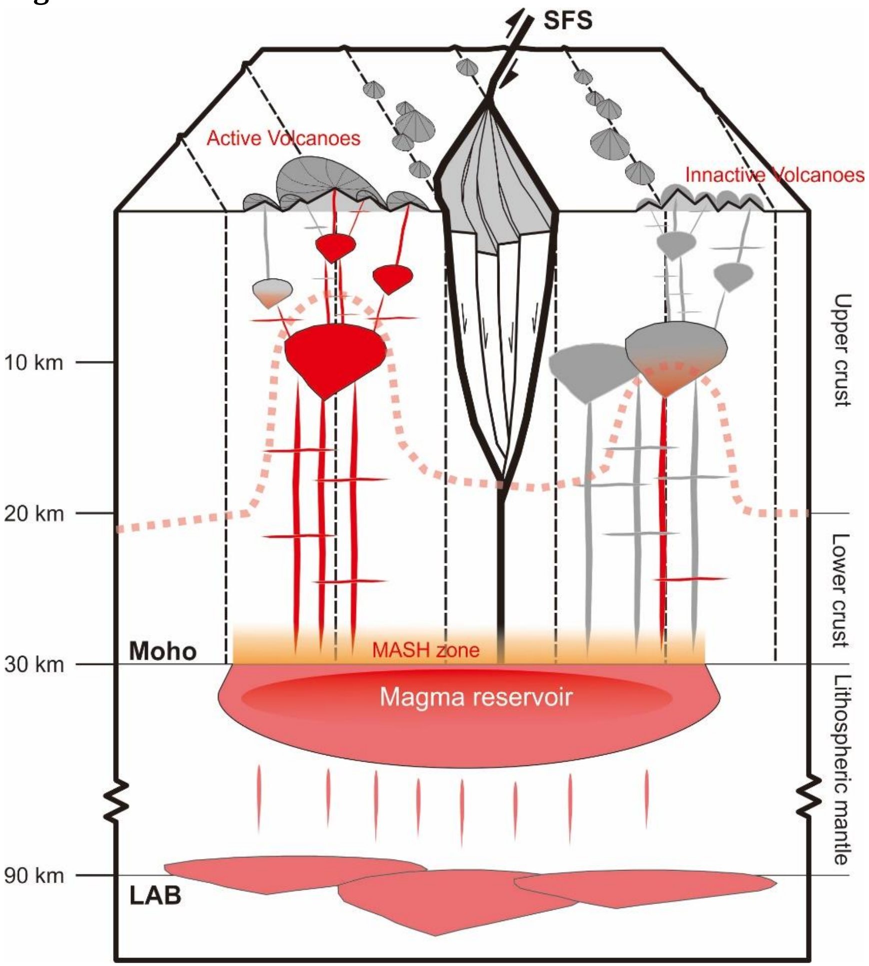
SFS
Active Volcanoes
Innactive Volcanoes
10 km
20 km
Moho
30 km
MASH zone
Magma reservoir
90 km
LAB
Upper crust
Lower crust
Lithospheric mantle

Figure-11.

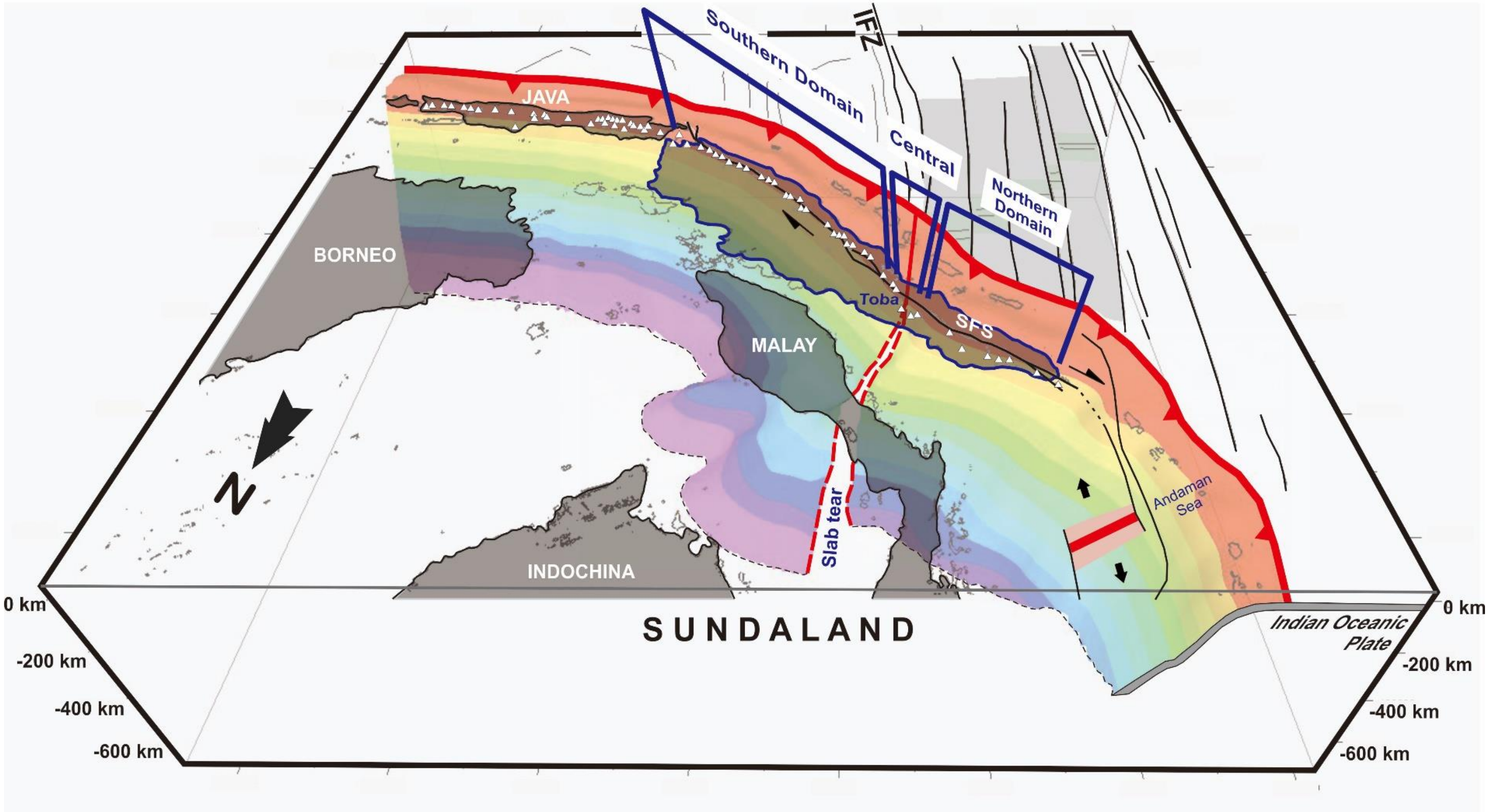

Southern Domain
IFZ
Central
Northern Domain
JAVA
BORNEO
Toba
SFS
MALAY
N
Slab tear
Andaman Sea
INDOCHINA
SUNDALAND
Indian Oceanic Plate
0 km
-200 km
-400 km
-600 km
0 km
-200 km
-400 km
-600 km

Figure-12.

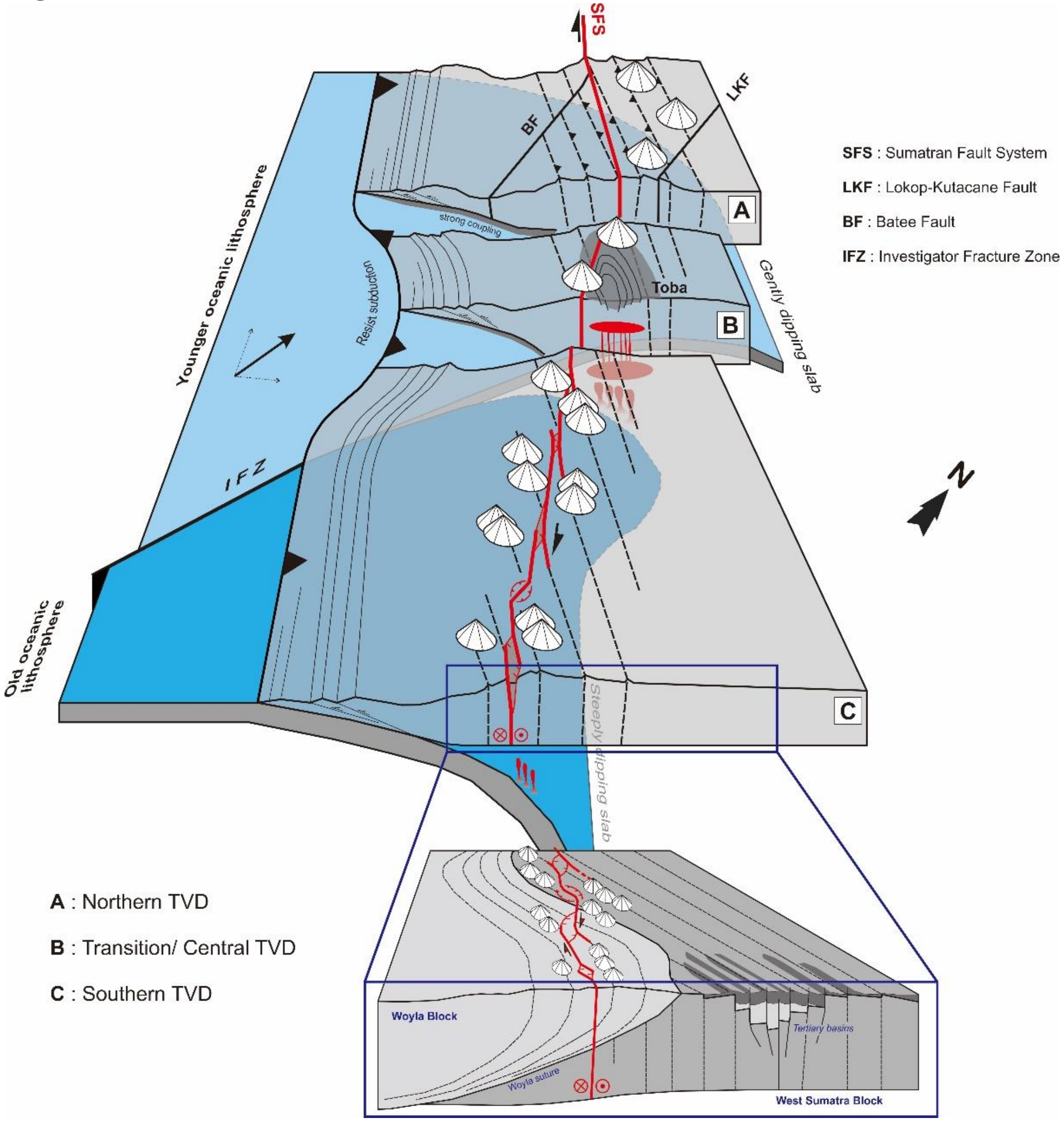

SFS
LKF
BF
SFS : Sumatran Fault System
LKF : Lokop-Kutacane Fault
BF : Batee Fault
IFZ : Investigator Fracture Zone
A
B
C
Toba
strong coupling
Resist subduction
Gently dipping slab
Younger oceanic lithosphere
IFZ
Old oceanic lithosphere
Steeply dipping slab
N
A : Northern TVD
B : Transition/ Central TVD
C : Southern TVD
Woyla Block
Woyla suture
Tertiary basins
West Sumatra Block

1133